

# Land use/land cover change and its impact on surface urban heat island and urban thermal comfort in a metropolitan city



Shahfahad<sup>a</sup>, Mohd Waseem Naikoo<sup>a</sup>, Abu Reza Md. Towfiqul Islam<sup>b</sup>, Javed Mallick<sup>c</sup>, Atiqur Rahman<sup>a,\*</sup>

<sup>a</sup> Department of Geography, Faculty of Natural Sciences, Jamia Millia Islamia, New Delhi 110025, India

<sup>b</sup> Department of Disaster Management, Begum Rokeya University, Rangpur 5400, Bangladesh

<sup>c</sup> Department of Civil Engineering, College of Engineering, King Khalid University, Abha, Saudi Arabia

## ARTICLE INFO

### Keywords:

Urban expansion  
Surface urban heat island intensity  
Urban thermal field variation index  
Thermal comfort  
Geographically weighted regression

## ABSTRACT

The increasing urban heat island intensity (UHII) is a matter of concern for the sustainable urban planning and maintaining urban thermal comfort in the metropolitan cities of developing countries like India. Therefore, in the current research, the land use/land cover (LU/LC) change and its impact on the surface UHI intensity (SUHII) and urban thermal comfort has been analyzed using Landsat datasets and geographically weighted regression (GWR) in Delhi metropolitan city. The result shows that the built-up area has increased from 315.18 to 720.24 sq. km in Delhi during 1991 to 2018 while other LU/LC types have declined. This has resulted in a substantial increase in LST and SUHII. The minimum, maximum and mean SUHII has increased by 1.26 °C, 4.6 °C and 1.18 °C during 1991 to 2018 and hence, the thermal comfort has declined in the city. The GWR analysis showed that the performance of GWR model was very good in showing the association between LU/LC and SUHII and the LU/LC pattern has significant impact on SUHII. The outcome of this research can be utilized for the formulation of SUHI mitigation strategies and maintaining urban thermal comfort in Delhi and cities with similar geographical conditions.

## 1. Introduction

During the last few decades, the urban population of the world has increased at a faster rate (Seto et al., 2012). The cities across the world experienced a growth of about 1.5% per year during 200–2015, while the rate of urban growth was about 2.6% per year in the developing countries (WUP, 2018). This increase in the urban population leads to the large-scale modification of the urban land use/land cover (LU/LC) pattern which ultimately creates several environmental and ecological problems (Aylett et al., 2016; Buo et al., 2021). The changing LU/LC pattern in urban areas also affects the quality of life in urban areas by altering its environment, deteriorating air quality and increasing the frequency of extreme climatic events like high-intensity rainfall, development of urban heat islands (UHI) and smog-like conditions (Naim and Kafy, 2021; Sahoo et al., 2020; McDonald et al., 2013; Rahman et al., 2011).

**Abbreviations:** SUHII, Surface urban heat island intensity; LU/LC, Land use/land cover; UTFVI, Urban thermal field variation index; NCT, National Capital Territory; LPG, Liberalisation, Privatisation and Globalisation; LST, Land surface temperature; GWR, Geographically weighted regression.

\* Corresponding author.

E-mail addresses: [fahadshah921@gmail.com](mailto:fahadshah921@gmail.com) (Shahfahad), [waseemnaik750@gmail.com](mailto:waseemnaik750@gmail.com) (M.W. Naikoo), [towfiq\\_dm@brur.ac.bd](mailto:towfiq_dm@brur.ac.bd) (A.R.Md. Towfiqul Islam), [jmallick@kku.edu.sa](mailto:jmallick@kku.edu.sa) (J. Mallick), [arahanm2@jmi.ac.in](mailto:arahanm2@jmi.ac.in) (A. Rahman).

<https://doi.org/10.1016/j.uclim.2021.101052>

Received 1 September 2021; Received in revised form 23 November 2021; Accepted 9 December 2021

Available online 16 December 2021

2212-0955/© 2021 Elsevier B.V. All rights reserved.

Therefore, the LU/LC change is one of the most prominent factors to be considered in urban planning, landscape management and environmental management (Hersperger et al., 2018; Panagopoulos et al., 2016). The haphazard changes in urban LU/LC pattern in the cities of developing countries lead to changes in thermal properties of the land surface (Liu et al., 2018) which leads to the increase in the surface UHI intensity (SUHII) over the urban areas (Yao et al., 2017; Munslow and O'Dempsey, 2010).

The concept of SUHI is a well-recognised phenomenon in urban environment studies (Parlow et al., 2021; Corburn, 2009). The SUHI is conspicuous with the higher surface temperature in urban areas vis-a-vis contiguous rural areas (Yao et al., 2019; Oke, 1973). The SUHII is an important aspect of the modelling of surface energy balance, urban thermal comfort and climate change at different scales (Li et al., 2018; Lee et al., 2012). The intensification of urban temperature is investigated by the rapid urbanization and industrialisation (Chun and Guldmann, 2014), LU/LC changes (Atasoy, 2020), increased impervious surfaces with surface biophysical differentiations and street design (Estoque et al., 2016) and increased energy consumptions (Giridharan and Emmanuel, 2018). The increasing SUHII, in turn, has resulted in increased frequency of heatwaves (Ward et al., 2016), atmospheric pollution (Cao et al., 2016), human health problems (Heaviside et al., 2017) and groundwater depletion due to accelerated water usage (Zhu et al., 2015). The vulnerability of the urban population to the SUHI can be investigated by quantifying and delineating the areas of thermal comfort and discomfort within an urban area (Guha et al., 2018). For this, the researchers have adopted an index called urban thermal field variation index (UTFVI) which is an indicator of urban thermal comfort (Naim and Kafy, 2021). The UTFVI delineates an urban area into various thermal comfort zones based on the conditions of heating and cooling (Shahfahad et al., 2021a).

The studies on UHI were initially based on the differences in rural and urban temperature (Ünal et al., 2019). The first shift in perspective of UHI studies was taken place in the first decade of the 21st century, when, Zhang (2006) proposed an index for analysing the thermal comfort of urban areas based on the UHII. Similarly, Xu et al., (2013) proposed an index for the UHII studies based on the relative temperature difference in the urban areas. Further, Ma et al. (2010) used the mean urban temperature as the criteria for the delineating of UHI. The other aspects of UHI studies such as the factors of its formation, consequences and mitigation strategies have also experienced a shift during the last few decades. For example, Wang and Akbari (2016) stressed the plantation of trees along the urban transport lines for the mitigation of SUHII in Montreal. Similarly, Akbari et al. (2009) analyzed the role of surface albedo on the SUHI formation and pointed that the SUHI can be mitigated by increasing the albedo of building and urban surfaces. Recently, some researchers analyzed the impact of coronavirus lockdown on the SUHII in different cities of the world and noted that the lockdown

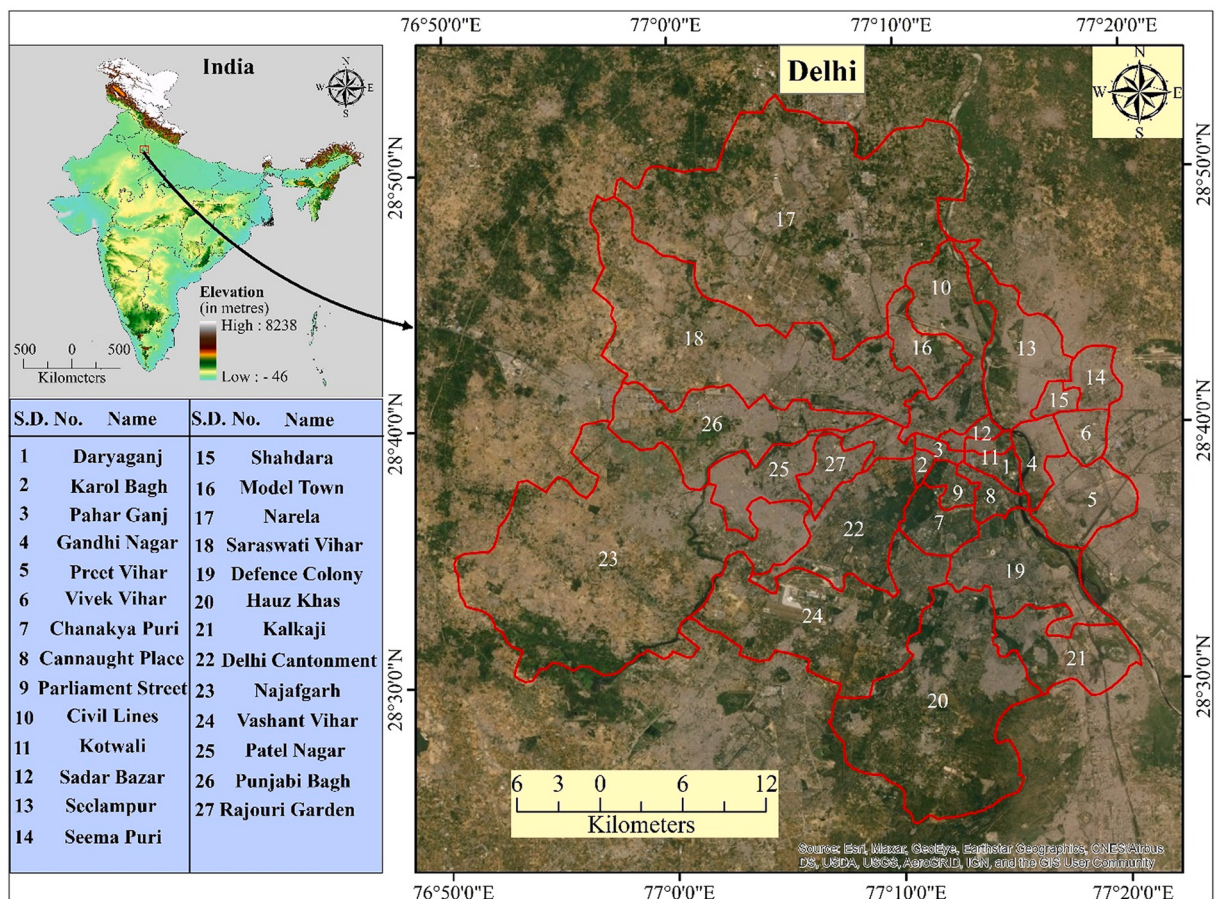


Fig. 1. Location and sub-district divisions of Delhi metropolitan city.

induced breakdown in the urban movement led to a significant decline in SUHII in cities (Ali et al., 2021; Chakraborty et al., 2021; Alqasemi et al., 2021).

Studies have been done on UHI of the Indian cities (Sahoo et al., 2020; Singh et al., 2014; Mohan et al., 2013; Mallick et al., 2013). Further, studies have also been done to analyze and quantify the SUHI of the Indian cities like Kolkata (Halder et al., 2021; Chatterjee et al., 2019), Mumbai (Shahfahad et al., 2021b), Delhi (Kumari et al., 2020a; Pandey et al., 2014; Mohan et al., 2013), Chennai (Rajan and Amirtham, 2021) etc. A few studies have been also done on the urban thermal comfort, but these studies are limited to the medium sized cities of India (Sharma et al., 2021; Ali and Patnaik, 2018). But the studies have not been done to analyze the urban thermal comfort of big metropolitan cities like Delhi. Therefore, NCT of Delhi has been rightly chosen to assess the urban thermal comfort and SUHII in response to changing LU/LC pattern during 1991 to 2018. The NCT of Delhi has experienced rapid transformation of its LU/LC pattern, especially after the economic reforms of 1991 (Chadchan and Shankar, 2012) popularly known as liberalization, privatization, globalization (LPG). This transformation of LU/LC pattern in Delhi has significantly affected the thermal environment of Delhi.

## 2. Material and methods

### 2.1. Description of the study area

The NCT of Delhi is located in the central part of India between 28° 24' 17" N & 28° 53' 00" N latitude and 76° 50' 00" E & 77° 20' 37" E longitude. The city has been divided into 11 districts and 27 sub-districts or tehsils (Fig. 1). In 2011, the population of Delhi was about 16.8 million and according to an estimate by World Urbanization Prospects (WUP, 2018), the population of Delhi was about 29 million in 2018. By 2030, the city is expected to be the world's most populous city, leaving behind Tokyo. The climate of Delhi varies from tropical moist type (Koppen–Cwa) to the semi-arid type (Koppen – Bsh) which gets influenced by the prevalence of continental air in the region (Rahman et al., 2011). The highest temperature of the city reaches about 45 °C during June whereas it goes down to nearly 2 °C in the month of December–January. The mean annual rainfall of Delhi is 800 cm, which occurs mostly during July–September due to the southwest monsoon.

With nearly 22% of its area under vegetation cover, Delhi is considered one of the greenest capital cities in the world (Chaudhry et al., 2011; Ramaiah and Avtar, 2019). Although the urban impervious surfaces dominate the landscape composition of the NCT of Delhi, the city has extensive vegetation cover. The vegetation cover in Delhi is both naturally vegetated areas as well as managed green spaces such as public parks, historical sites, educational institutions, and others (Wentz et al., 2008). Due to its long history since medieval times, the city has a juxtaposition of planned and unplanned areas. The areas developed during medieval times by the rulers of the Delhi Sultanate and Mughal period are congested and lacks open and green spaces while the areas developed during the British rule are well planned and have adequate open and green spaces (Paul and Nagendra, 2015). The areas developed in the post-independence era (after 1947) are also congested and do not have adequate open and green spaces due to a lack of planning.

### 2.2. Material used in the study

The data used in this study comprises Landsat datasets, topographical map of India and a sub-district level map of India from the handbook of the Census of India (2011). The Landsat datasets were downloaded from the United States Geological Survey (USGS) website Earth Explorer (<https://earthexplorer.usgs.gov/>). The LU/LC maps of Delhi were prepared using the optical bands while the retrieval of LST and SUHII were done using the thermal bands of Landsat datasets (Table 1). The topographical map of India, taken from the Bhuvan portal of the National Remote Sensing Centre (NRSC) of India (<https://bhuvan-app1.nrsc.gov.in/bhuvan2d/bhuvan/bhuvan2d.php>) was used to extract the shapefile of India and Delhi, while the sub-district level division of Delhi was extracted using the map taken from the Census of India handbook.

## 3. Methods

The downloaded Landsat data were pre-processed using the ERDAS Imagine software (2014 version). The pre-processing steps performed in this study were layer stacking of the satellite data, atmospheric and radiometric reduction (like haze and noise reduction) and creation of subset layers using the shapefile of Delhi taken from the Bhuvan portal. The LU/LC classification was done using the K-

**Table 1**

Details of the Landsat data used.

Satellite/Sensor	Date of acquisition	Path/Row	Bands used	Cloud Cover (in %)	Thermal constants (K value)		Sun elevation (in degrees)	Sun Azimuth (in degrees)
					K1	K2		
Landsat 5 (TM)	14-Mar-1991	146/40	2, 3, 4 & 6	0.00	607.76	1260.56	44.310	127.908
Landsat 7 (ETM+)	02-Apr-2001	146/40	2, 3, 4 & 6	0.00	666.09	1282.71	55.818	129.519
Landsat 5 (TM)	06-Apr-2011	146/40	2, 3, 4 & 6	1.00	607.76	1260.56	56.950	128.071
Landsat 8 (OLI/TIRS)	31-Mar-2018	146/40	3, 4, 5 & 10	0.01	774.8853	1321.0789	56.657	133.485

means clustering classifier on the open-source QGIS software (version 3.14) and then accuracy assessment was done using the 500 samples collected from field visits as well as through Google Earth pro. The sample points were collected for the same locations in classified maps as well as ground in such a way that it covers all the LU/LC types in a proportion of their area. Furthermore, the field samples were not available for 1991, 2001 and 2011 hence, the samples of these years were taken through Google earth pro. The LST retrieval was done using the thermal bands of the Landsat datasets using the mono-window algorithm and then SUHII and UTFVI were modelled using it. Finally, the association between UHII and LU/LC pattern was calculated using geographically weighted regression (GWR) technique to assess the impacts on LU/LC change on the SUHII.

### 3.1. LU/LC classification and accuracy assessment

Various LU/LC classification techniques and approaches have been used during the recent past using satellite datasets such as neural networks, maximum likelihood classifier, K-means clustering, indices overlay method, etc. (Kumari et al., 2021; Al-Kafy et al., 2020; Talukdar et al., 2020). In the present study, we used the K-means clustering based unsupervised classification technique for the LU/LC mapping of Delhi. The composite of the optical bands of Landsat datasets (band 2, 3 & 4 in Landsat 5 & 7 while band 3, 4 & 5 in Landsat 8) were utilized for the LU/LC classification. Six LU/LC classes were identified in Delhi based on the level-I LU/LC classification system of the National Remote Sensing Center (NRSC) i.e. built-up area, open land, vegetation cover, cropland water bodies, and scrubland (**Table 2**).

The assessment of classification accuracy was done to validate the accuracy of classified maps and evaluate the performance of the classifier used. In this study, the kappa coefficient was applied to analyze the classification accuracy of the LU/LC maps using 500 randomly chosen points of the same locations on the classified maps as well as from the field or Google Earth. The evidence from previous literature suggests that a classification accuracy above 80% makes good agreement between classified LU/LC maps and ground reality (Meng et al., 2021; Dutta et al., 2021). The results of the Kappa coefficient shows that overall accuracy was more than 90% for each classified map (**Table 3**).

### 3.2. Retrieval of land surface temperature (LST)

In this study, the mono-window algorithm was applied for the retrieval of LST (Qin et al., 2001; Sobrino et al., 2004; Kumari et al., 2020b). The LST retrieval using Landsat datasets involves four steps i.e. conversion of the DN value to the spectral radiance ( $L_\lambda$ ), the conversion of spectral radiance to brightness temperature (BT), correction of emissivity through the proportion of vegetation (Pv) then LST retrieval (Yao et al., 2021; Du et al., 2020; Fan et al., 2017).

The conversion of DN value to the spectral radiance from Landsat 5 & Landsat 7 was done using Eq. (1).

$$L_\lambda = \left\{ \frac{L_{MAX\lambda} - L_{MIN\lambda}}{Q_{CalMAX} - Q_{CalMIN}} \right\} (Q_{Cal} - Q_{CalMIN}) + L_{MIN\lambda} \quad (1)$$

where  $L_\lambda$  representsspectral radiance,  $L_{MAX\lambda}$  and  $L_{MIN\lambda}$  represent spectral radiance of the sensor of satellite scaled to the  $Q_{CalMAX}$  &  $Q_{CalMIN}$ , respectively, while  $Q_{Cal}$  represents the calibrated quantized pixel value.

The conversion of DN value of Landsat 8 into the spectral radiance was done using Eq. (2).

$$L_\lambda = M_L \times Q_{Cal} + A_L \quad (2)$$

where  $L_\lambda$  represents spectral radiance,  $M_L$  represents the explicit multiplicative rescaling factor of the thermal band,  $Q_{Cal}$  represents the calibrated quantized pixel value, while  $A_L$  represents the additive rescaling factor of the thermal band.

The retrieval of brightness temperature using the calibration constant at the Top-of-Atmosphere was done using Eq. (3).

$$B_T = \frac{K_2}{\ln \left( \frac{K_1}{L_\lambda} + 1 \right)} \quad (3)$$

where  $B_T$  represents the brightness temperature (kelvin),  $L_\lambda$  represents radiance, while  $K_1$  and  $K_2$  are the thermal calibration constant taken from metadata (**Table 1**).

For emissivity correction, the NDVI threshold technique of Sobrino et al. (2004) was used. Thus, firstly, the proportion of vegetation

**Table 2**

Description of the LU/LC classes identified in Delhi based on NRSC (1995) scheme.

S. no	LU/LC class	Description of the LU/LC class
1	Built-up area	Residential, commercial, industrial and other infrastructural structures
2	Open land	Bare soil without any natural or manmade cover like barren land and waste land
3	Vegetation	Dense vegetated areas like forest, plantation and trees along roads & water bodies
4	Scrubland	Grasslands, orchards and recreational areas with sparse green cover like parks and lawns
5	Cropland	All cultivated lands
6	Water body	Rivers, canals, lakes, ponds and wetlands

**Table 3**

Accuracy assessment of LU/LC maps using Kappa coefficient.

Year	User's accuracy (%)	Producer's accuracy (%)	Overall accuracy (%)	Kappa coefficient (%)
1991	94.46	83.34	91.13	0.934
2001	95.62	84.59	90.28	0.924
2011	96.31	85.59	92.23	0.941
2018	96.37	86.48	94.26	0.925

$(P_V)$  was calculated using Eq. (4).

$$P_V = \left[ \frac{NDVI - NDVI_{min}}{NDVI_{max} - NDVI_{min}} \right]^2 \quad (4)$$

In the next step, the emissivity ( $\epsilon$ ) was corrected using the Eq. (5).

$$\epsilon = 0.004P_V + 0.986 \quad (5)$$

For Landsat 8 the emissivity correction was done using a modified equation (Eq. (6)) was used by Yu et al. (2014).

$$\epsilon = 0.00149P_V + 0.98481 \quad (6)$$

The LST was finally calculated following Artis and Carnahan (1982) using Eq. (7).

$$T = \left[ \frac{B_T}{1 + \left( \lambda \times \frac{B_T}{P} \right) \ln(\epsilon)} \right] \quad (7)$$

where, T refers to the retrieved LST in Kelvin, TB refers to brightness temperature,  $\lambda$  expresses the wavelength of radiance emitted,  $P = h \times c / s$ ; in which  $h$  represents Planck's constant ( $6.624 \times 10^{-34}$  J s),  $c$  represents velocity of the light ( $2.998 \times 10^8$  m/s), while  $s$  represents Boltzmann constant ( $1.38 \times 10^{-23}$  J/K) and  $\epsilon$  refers to the corrected emissivity.

For the validation of LST retrieved, in-situ data were not available. As a result, the MODIS Aqua LST data products were used for the validation of LST retrieved from Landsat datasets of 2001, 2011, and 2018. In this study, 600 sample points were randomly selected from the MODIS LST data product and the retrieved LST for the same site, and the correlation between the two was computed, as well as the LST gap. A very strong and positive correlation between the LST retrieved and the MODIS LST was found i.e. 0.93, 0.89, and 0.94 for 2001, 2011 and 2018 respectively. The average LST gap was 1.2 °C, 1.6 °C, and 0.9 °C for 2001, 2011, and 2018 respectively.

### 3.3. Modelling surface urban heat island intensity (SUHII)

The most common technique used for modelling the impact of urban expansion and LU/LC change on SUHII is to measure the difference between the urban and rural temperatures (Ünal et al., 2019). However, in the context of local climate zone (LCZ) concept, the SUHII has been defined as the difference between the LST of built-up areas and green space (Bechtel et al., 2019; Stewart and Oke, 2012). As the LST of green areas also show variation, the average LST over green area (i.e. scrublands, dense and sparse vegetation and grasslands) is taken as the reference temperature for the SUHII mapping. Thus, the SUHII at each built-up pixel was calculated using Eq. (8).

$$SUHII_i = T_{bu_i} - T_{gs} \quad (8)$$

where, the  $SUHII_i$  is the SUHII at built-up pixel  $i$ ,  $T_{bu_i}$  is the LST at built-up pixel  $i$  and  $T_{gs}$  is the mean LST of the green space pixels. The SUHII of the study area was further derived as following (Eq. (9)).

$$SUHII = \frac{1}{n} \sum_{i=1}^n SUHII_i \quad (9)$$

where,  $SUHII_i$  represents the SUHII at pixel  $i$  and  $n$  represents total number of built-up pixels.

Following Lu et al., (2020), we classified the SUHII maps into 5 classes i.e. no SUHII (<0.00), low SUHII (0.00–2.00), moderate SUHII (2.00–4.00), high SUHII (4.00–6.00) and very high or extreme SUHII (>6.00).

### 3.4. Modelling urban thermal comfort using UTFVI

For the modelling of urban thermal comfort, the ecological evaluation index (EEI) was created using the UTFVI (Eq. (10)). The UTFVI technique is based on the relative temperature difference technique of Xu et al., (2013).

$$UTFVI = \frac{T_s - T_{mean}}{T_{mean}} \quad (10)$$

The EES created using UTFVI divided the urban areas into six thermal comfort zones for the human being from worst to excellent ([Table 4](#)).

### 3.5. Calculation of association between SUHII and LU/LC pattern

To analyze the relationships between UHII and LU/LC patterns, we applied the geographically weighted regression (GWR). The advantage of using GWR is that it does not only reveals the relationships between two variables but also models the spatial variation in their relationships ([Fotheringham et al., 2003](#)). Further, it outspreads the global regression by incorporating the locational parameters to create local coefficients to explain the spatial non-stationarity. Mathematically, the GWR expresses as the Eq. [\(11\)](#).

$$y_i = \beta_0(u_i, v_i) + \sum_{j=1}^n \beta_j(u_i, v_i)x_{ij} + \varepsilon_i \quad (11)$$

Where,  $y_i$  represents the dependent variable i.e. SUHII in this study,  $x_{ij}$  represents the  $j$ th independent variable at the  $i$ th location while  $\varepsilon_i$  represents the random error at the  $i$ th location.  $(u_i, v_i)$  represents coordinates of pragmatic location  $I$  while  $\beta_j(u_i, v_i)$  represents the coefficient of the  $j$ th variable at location  $i$ .

## 4. Results

### 4.1. Land use/land cover (LU/LC) pattern and change (1991–2018)

The LU/LC classification maps of Delhi shows a consistent increase in the built-up area 1991–2018 ([Fig. 2](#)) which is common in the metropolitan cities of developing countries. The concentration of built-up area was maximum in the core of the city in 1991, which has gradually increased and expanded to the outskirts of the city. At the same time, the cropland and scrublands have declined significantly. The result shows an interesting three-tier pattern in the LU/LC change, i.e. the scrublands and croplands firstly converts to the open land and then into the built-up surface. The croplands and scrublands in 1991 were converted into open land in 2001 but they were converted into built-up areas in 2011. In 2018, the built-up areas get further densified ([Fig. 2](#)). The maximum expansion of built-up areas has occurred in the north and south-western sub-districts (particularly in Narela, Najafgarh, Patel Nagar and Saraswati Vihar). At the same time, the built-up areas have also increased in the sub-districts of south Delhi like Kalkaji, Vasant Vihar and Hauz Khas. The vegetation cover has experienced a significant decline during 1991–2001 in the north-central and south-central sub-districts like Civil Lines, Rajouri Garden and Delhi Cantonment, but has increased during 2001–11 and 2011–18.

[Table 5](#) presents the statistics of the LU/LC pattern in Delhi during 1991–2018. It can be noticed that the area under built-up surface has increased to more than double (from 315.18 in 1991 to 720.24 sq. km in 2018). But the cropland, water bodies, vegetation cover and open land has significantly declined in Delhi during 1991–2018. The scrubland shows a fluctuating trend as it declined from 189.90 to 154.12 sq. km during 1991–2001 while increased to 214.89 sq. km in 2011 and again declined to 190.33 sq. km in 2018. The vegetation cover, on the other hand, declined during the first decade of the study period but later on experienced a significant increase ([Table 5](#)). The reason behind this increase in vegetation cover is the large-scale greening drive in the interior parts of the city by the state government and local municipal corporations ([Paul and Nagendra, 2015](#); [Forest Department, 2014](#)).

The built-up area has experienced maximum expansion in the sub-districts of the western, northern and southern parts of Delhi like Najafgarh, Narela, Punjabi Bagh and Vasant Vihar, while it was least in the sub-districts of core areas of Delhi like Civil Lines, Daryaganj, Kotwali, Karol Bagh, Connaught Place and Shahdara. The reason behind the low increase of built-up areas in the sub-districts of the core areas is that the density of built-up area was already high in these sub-districts ([Appendix-I](#)). [Fig. 3](#) shows that the expansion of built-up surfaces has mostly occurred due to the conversion of cropland and scrubland to the built-up area in western and northern parts while it has occurred because of the conversion from open land in the southern parts. The transformation of cropland to the built-up area has occurred in almost all parts of Delhi, except eastern and central parts. At the same time, some sub-districts like Civil Lines, Parliament Street and Connaught Place have experienced a very low increase in the built-up surface because these are planned sub-districts where further developmental works are restricted. Furthermore, it can be noticed from [Fig. 3](#) that the croplands and scrublands have been converted firstly to the open land, especially during 1991–2001 and then to the built-up area during 2001–11 and 2011–18. The change matrix also shows that the biggest contributor to the expansion of the built-up area in Delhi was open land, while the scrubland and croplands were the biggest contributors to the open land ([Table 6](#)).

**Table 4**

Classification of urban thermal ecology based on threshold values of UTFVI based on [Ma et al. \(2010\)](#).

UTFVI	Urban heat island (UHI) phenomenon	Ecological Evaluation Index (EEI)	Delhi (Area in %)			
			1991	2001	2011	2018
<0	None	Excellent	45.97	48.32	48.01	50.01
0.000–0.005	Weak	Good	0.00	0.00	0.00	3.90
0.005–0.010	Moderate	Normal	16.15	7.44	0.00	3.50
0.015–0.015	Strong	Bad	0.00	0.00	16.16	3.29
0.015–0.020	Stronger	Worse	0.00	0.00	0.00	3.06
> 0.020	Strongest	Worst	37.87	44.23	35.83	36.24

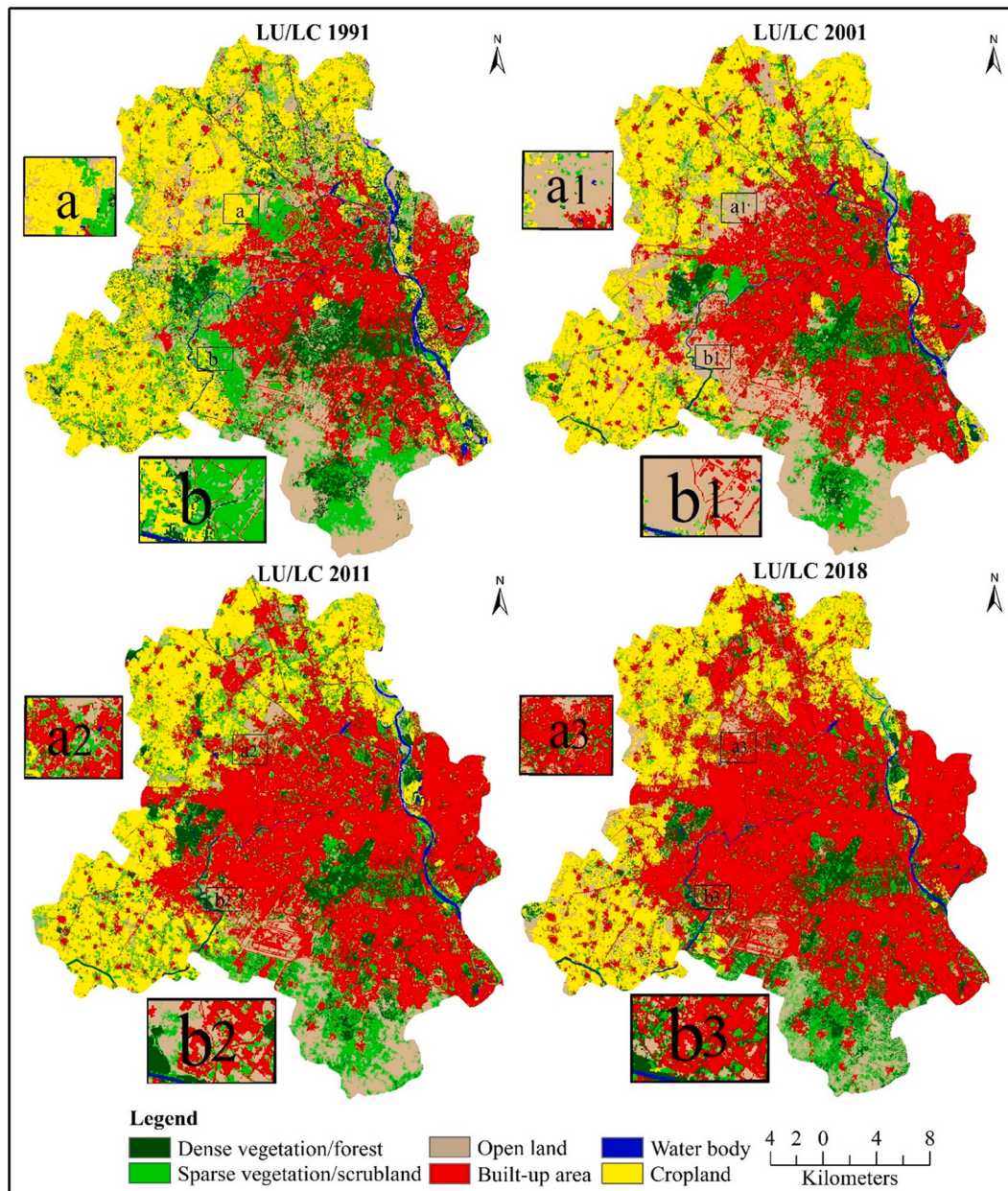


**Fig. 2.** Land use/land cover (LU/LC) pattern in Delhi during 1991–2018.

**Table 5**

Land use/land cover (LU/LC) variation in Delhi during 1991–2018.

LU/LC Class	1991		2001		2011		2018	
	Area in sq. km	Area in %	Area in sq. km	Area in %	Area in sq. km	Area in %	Area in sq. km	Area in %
Built-up area	315.18	21.23	498.26	33.56	623.96	42.03	720.24	48.51
Open land	322.37	21.71	309.60	20.85	172.69	11.63	155.98	10.51
Vegetation	205.54	13.84	109.57	7.38	122.73	8.27	140.79	9.48
Scrubland	189.10	12.74	154.12	10.38	214.89	14.47	190.33	12.82
Cropland	433.05	29.17	398.04	26.81	335.73	22.61	264.16	17.79
Water bodies	19.43	1.31	15.08	1.02	14.67	0.99	13.17	0.89
Total	1484.67	100	1484.67	100	1484.67	100	1484.67	100

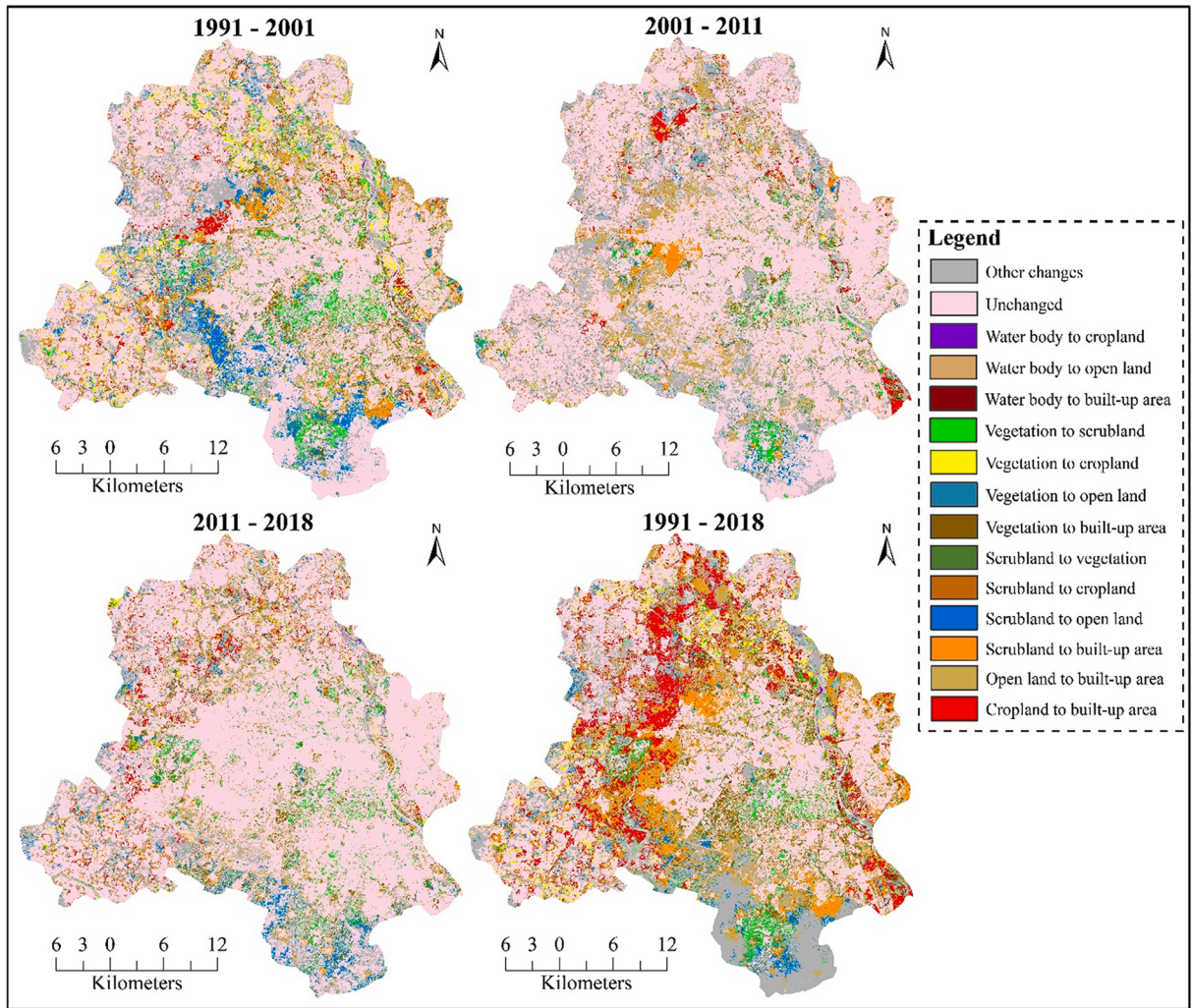


**Fig. 3.** Pattern of land use/land cover (LU/LC) change in Delhi during 1991–2018.

#### 4.2. Variation in LST during 1991–2018

The study shows that LST for Delhi varies between 17.70 and 30.25 °C in 1991; 19.16 to 34.78 °C in 2001; 19.87 to 34.60 °C in 2011 & 23.86 to 38.99 °C in 2018. From the analysis of LST, it was found that the spatial distribution of high LST has a shifting pattern (Fig. 4). The patches of high LST can be noticed in all sub-districts of Delhi in 1991, although it was higher in the southern sub-districts, especially in Hauz Khas and Vasant Vihar sub-districts. The LST is moderate in the central sub-districts in 1991 but is low in the eastern part over the Yamuna River bed as well as northern parts (in Narela, Civil Lines and Model Town sub-districts). In 2001, the patches of higher LST increased in the southern and western sub-districts of Delhi, although, it declined from the northern and north-western sub-districts. The most noticeable change in the pattern of LST can be seen in 2011 where the clusters of higher LST increased significantly in the central sub-districts while it declined in the outskirts of the city, especially in northern and south-western sub-districts. This is because of the increase in vegetation cover in the outskirts of Delhi (Paul and Nagendra, 2015) which has resulted in comparatively lower LST in the south-western and northern parts than the central parts of Delhi. In 2018, the LST again increased in the sub-districts of western, south-western and northern parts of Delhi like Najafgarh, Narela, and Saraswati Vihar due to the expansion of the built-up area in these sub-districts.

The district-wise variation in the statistics of LST shows that the LST has increased in almost all the sub-districts of Delhi during 1991–2018. The minimum LST was below 20 °C in all the sub-districts of Delhi in 1991 except Pahar Ganj and Parliament Street which increased to more than 25 °C in 2018 in most of the sub-districts (Fig. 5). Similarly, the maximum LST was below 30 °C in all the sub-districts except Kalkaji in 1991 which increased to more than 35 °C in most of the sub-districts in 2018. The highest increase in maximum LST was noted from the sub-districts of western parts like Model Town & Najafgarh and eastern parts like Preet Vihar. The increase in maximum LST was also very high in the central parts like in Delhi Cantonment. The mean LST at the same time shows very

**Table 6**  
Land use/land cover change matrix.

		2001 (Sq. km)					
		Built-up area	Open land	Vegetation	Scrubland	Cropland	Water bodies
1991 (Sq. km)	Built-up area	<b>305.74</b>	1.73	1.09	0.79	0.00	0.00
	Open land	79.31	<b>157.47</b>	15.47	39.38	31.9	1.87
	Vegetation	39.00	24.41	<b>65.87</b>	39.02	34.13	1.76
	Scrubland	49.62	63.65	12.63	<b>37.06</b>	24.59	0.94
	Cropland	23.38	60.23	10.15	36.67	<b>306.47</b>	1.09
	Water bodies	1.21	2.11	4.36	1.2	0.95	<b>9.41</b>
	Total	498.26	309.6	109.57	154.12	398.04	15.08
		2011 (Sq. km)					
		Built-up area	Open land	Vegetation	Scrubland	Cropland	Water bodies
2001 (Sq. km)	Built-up area	<b>463.41</b>	10.78	1.89	15.36	0.00	0.24
	Open land	83.11	<b>107.69</b>	20.83	62.22	26.96	1.94
	Vegetation	20.90	7.15	<b>56.33</b>	19.74	6.24	1.85
	Scrubland	35.77	18.30	27.67	<b>64.53</b>	25.77	0.96
	Cropland	18.91	27.55	13.69	52.29	<b>276.41</b>	0.94
	Water bodies	1.86	1.22	2.32	0.75	0.35	<b>8.74</b>
	Total	623.96	178.02	122.73	214.89	335.73	14.67
		2018 (Sq. km)					
		Built-up area	Open land	Vegetation	Scrubland	Cropland	Water bodies
2011 (Sq. km)	Built-up area	<b>606.98</b>	2.11	0.80	1.19	0.00	0.00
	Open land	38.79	<b>66.01</b>	17.49	68.57	15.01	0.50
	Vegetation	14.40	8.82	<b>72.93</b>	21.03	5.40	2.64
	Scrubland	37.04	37.63	36.71	<b>76.39</b>	23.15	0.41
	Cropland	22.47	39.95	10.69	21.75	<b>220.04</b>	0.34
	Water bodies	0.56	1.46	2.17	1.40	0.56	<b>9.28</b>
	Total	720.24	155.98	140.79	190.33	264.16	13.17
		2018 (Sq. km)					
		Built-up area	Open land	Vegetation	Scrubland	Cropland	Water bodies
1991 (Sq. km)	Built-up area	<b>305.31</b>	1.80	3.36	0.56	0	0.00
	Open land	140.58	<b>65.09</b>	34.77	58.38	21.28	1.10
	Vegetation	80.75	12.43	<b>58.76</b>	26.68	12.73	1.71
	Scrubland	91.32	23.68	21.79	<b>67.62</b>	15.49	1.08
	Cropland	98.74	51.83	18.64	35.48	<b>213.63</b>	1.07
	Water bodies	3.54	1.15	3.47	1.61	1.03	<b>8.21</b>
	Total	720.24	155.98	140.79	135.81	264.16	13.17

high but uniform increase in almost all wards, although, during 2001–11, the mean LST decreased in almost all the sub-districts ([Fig. 5](#)). This decrease in mean LST can be linked to the increase in vegetation cover in Delhi during this period which significantly reduces the LST in an urbanized environment ([Zawadzka et al., 2021](#); [Wang and Akbari, 2016](#)). Further, the maximum LST shows a fluctuating pattern of increase and decrease in some sub-districts i.e. it increased during 1991–2001 but declined during 2001–11 and again increased during 2011–18.

#### 4.3. Variation in SUHII during 1991–2018

The analysis of [Fig. 6](#) shows that the SUHII is high in the outskirts of Delhi in comparison to the core areas. This is because the core areas of Delhi have healthy vegetation cover while the outskirt areas of Delhi had experienced large-scale haphazard expansion of the built-up surface during past few decades. At the same time, the open land in the outer parts of Delhi is in the form of exposed rocky surfaces of the residual Aravalli hills which gives rise to the SUHII ([Singh et al., 2014](#); [Mallick et al., 2013](#)). It can be noticed that the SUHII has significantly increased during 1991–2018 in Delhi, although it has variation in its distribution. In 1991, the SUHII was very low in Delhi in almost all parts and very high SUHII was completely absent from Delhi while high and moderate SUHII was clustered in the small pockets in south-western, northern and southern parts. But in 2001, an increase in the high and very high SUHII was noticed in south-western, southern and central parts of Delhi like in Kalkaji, Delhi Cantonment, Najafgarh, Vasant Vihar and Hauz Khas sub-districts. Further, the eastern and western sub-districts like Preet-Vihar, Vivek Vihar and Punjabi Bagh also noticed a significant increase in the high and very high SUHII. In 2011, the SUHII declined in the southern and central parts especially in Hauz Khas, Delhi Cantonment and Defence Colony sub-district, although the patches of high SUHII increased in the southern and south-western parts,

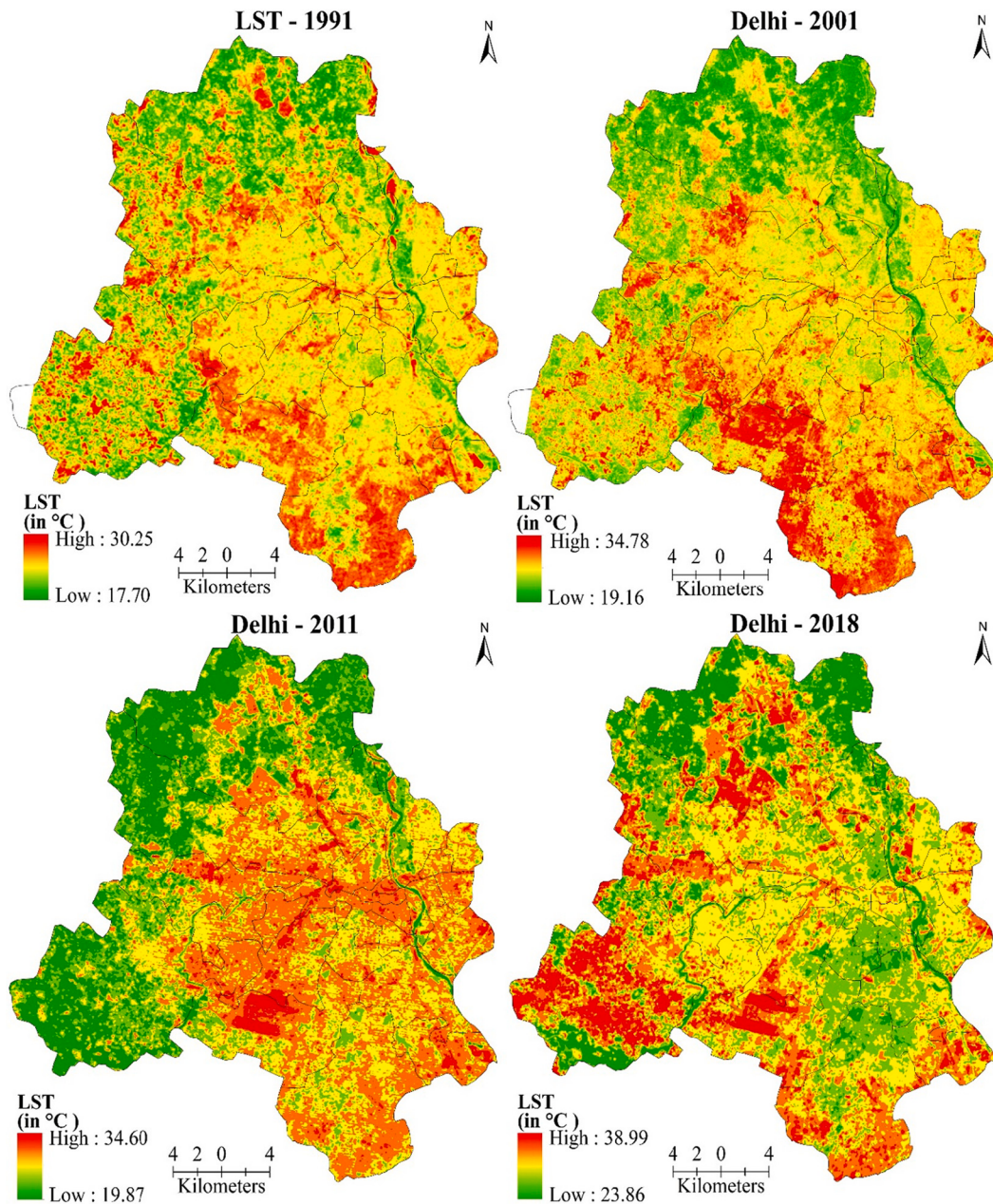


Fig. 4. Spatio-temporal dynamics of land surface temperature (LST) pattern in Delhi during 1991–2018.

especially over the Indira Gandhi International (IGI) airport as well as in the eastern parts of Delhi. The SUHII declined in the central parts in 2018 but it increased significantly in the south-western, southern and northern sub-districts of the city such as Najafgarh, Hauz Khas, Model Town and Narela (Fig. 6).

The areal coverage of very high, high and moderate SUHII has also increased in Delhi during 1991–2018 while the areal coverage of low and no SUHII has declined significantly (Table 7). In 1991, very high SUHII zones were absent in Delhi but in 2018, about 3.56% area of Delhi was under very high SUHII zone. The area under high SUHII was 0.01% of the total area in 1991 which increased to 5.75%. Similarly, the area under moderate and low SUHII also increased during 1991–2018 i.e. from 1.24 to 11.56% and 16.31 to 26.11% respectively. On the other hand, the area under no SUHII was 6.70% in 1991 which declined to 3.36% in 2018.

Fig. 7 shows the variation in SUHII over the different sub-districts of Delhi during 1991–2018. The result shows that the minimum SUHII was highest in 1991 in most of the sub-districts and it has declined in some of the sub-districts during the study period. However, it has increased in some sub-districts like Vasant Vihar, Chanakyapuri, Shahdara etc. The maximum SUHII shows a fluctuating pattern of increase and decrease, although it has increased in most of the sub-districts during 1991–2018. The maximum SUHII experienced an

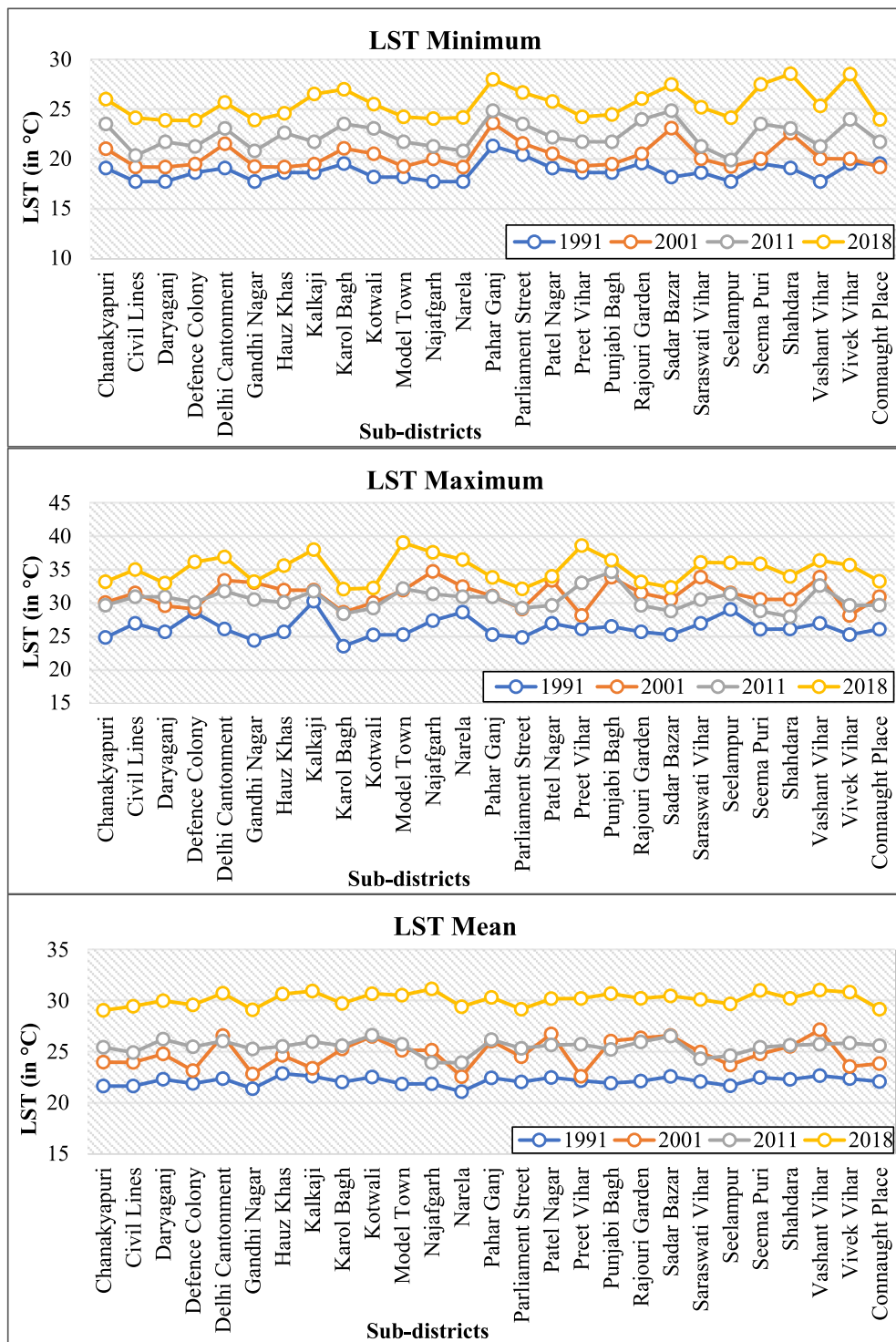
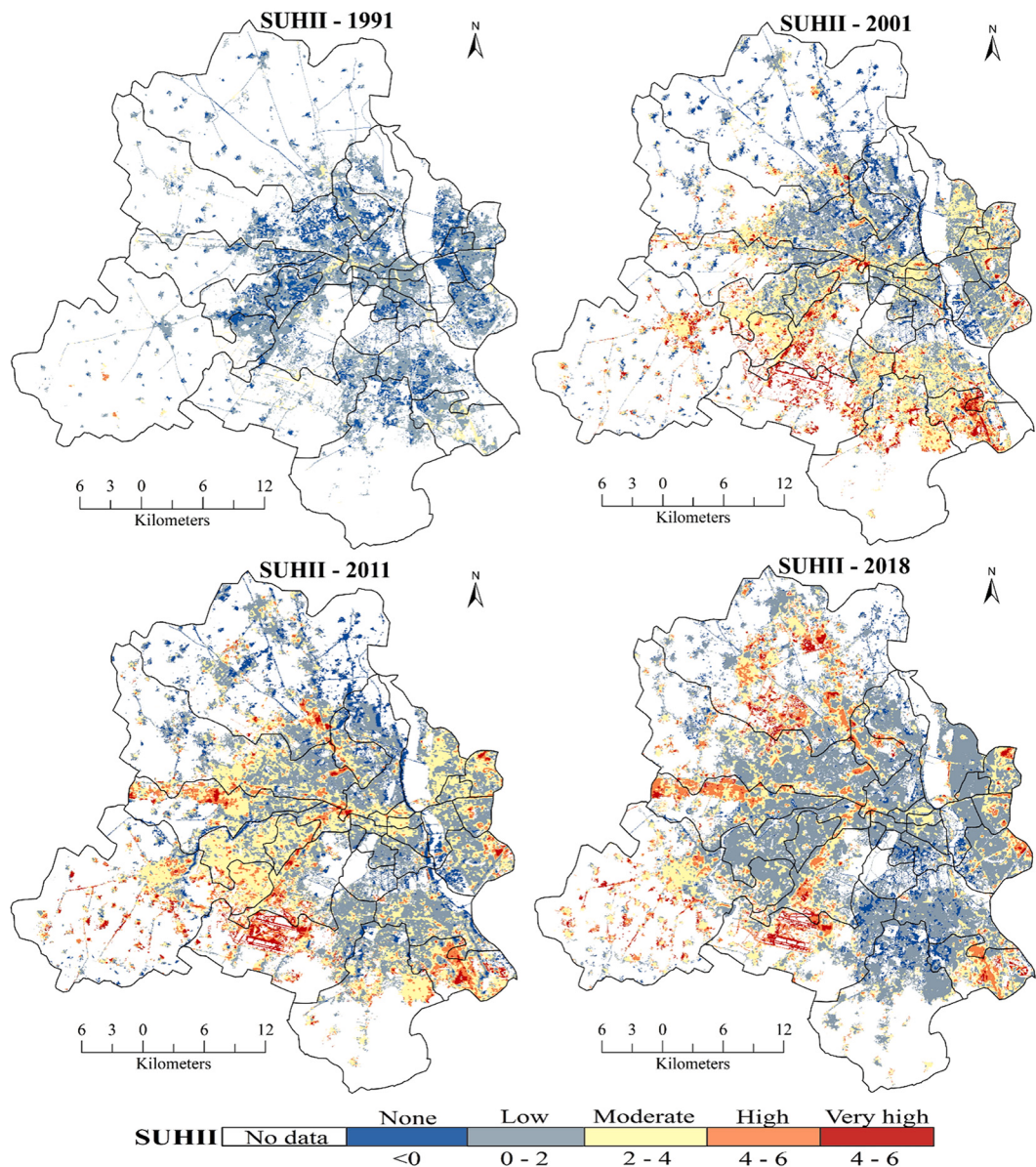


Fig. 5. Sub-district wise variation in statistics of LST in Delhi.

increase during 1991–2001 in most of the sub-districts but it declined during 2001–11 and again increased during 2011–18. The decline in maximum SUHII during 2001–11 can be linked to the increase in vegetation cover in Delhi due to the large-scale plantation drive by state government and municipal corporations during the preparation of the Commonwealth Games of 2010 (Baviskar, 2011). Overall, the maximum SUHII has increased during 1991–2018 and the highest increase was noted from the sub-districts of outer parts



**Fig. 6.** Spatio-temporal dynamics of SUHII (in °C) in Delhi during 1991–2018.

**Table 7**  
Spatio-temporal variation in the areal coverage of SUHII zones.

SUHII zones/Year	Area in percent			
	1991	2001	2011	2018
No Data	75.74	61.24	51.57	49.66
None/No SUHII	6.7	4.68	3.72	3.36
Low	16.31	13.49	18.52	26.11
Moderate	1.24	14.41	17.67	11.56
High	0.01	3.87	5.15	5.75
Very High	0	2.31	3.37	3.56

like Model Town, Preet Vihar, Najafgarh and Narela. While the sub-districts of core areas like Pahar Ganj, Civil Lines, Daryaganj etc. had experienced very low increase in maximum SUHII. On the other hand, the mean SUHII shows comparatively low fluctuation and a steady increase in most of the sub-districts. The sub-districts of outer parts like Najafgarh, Kalkaji, Punjabi Bagh, Rajouri Garden, etc.

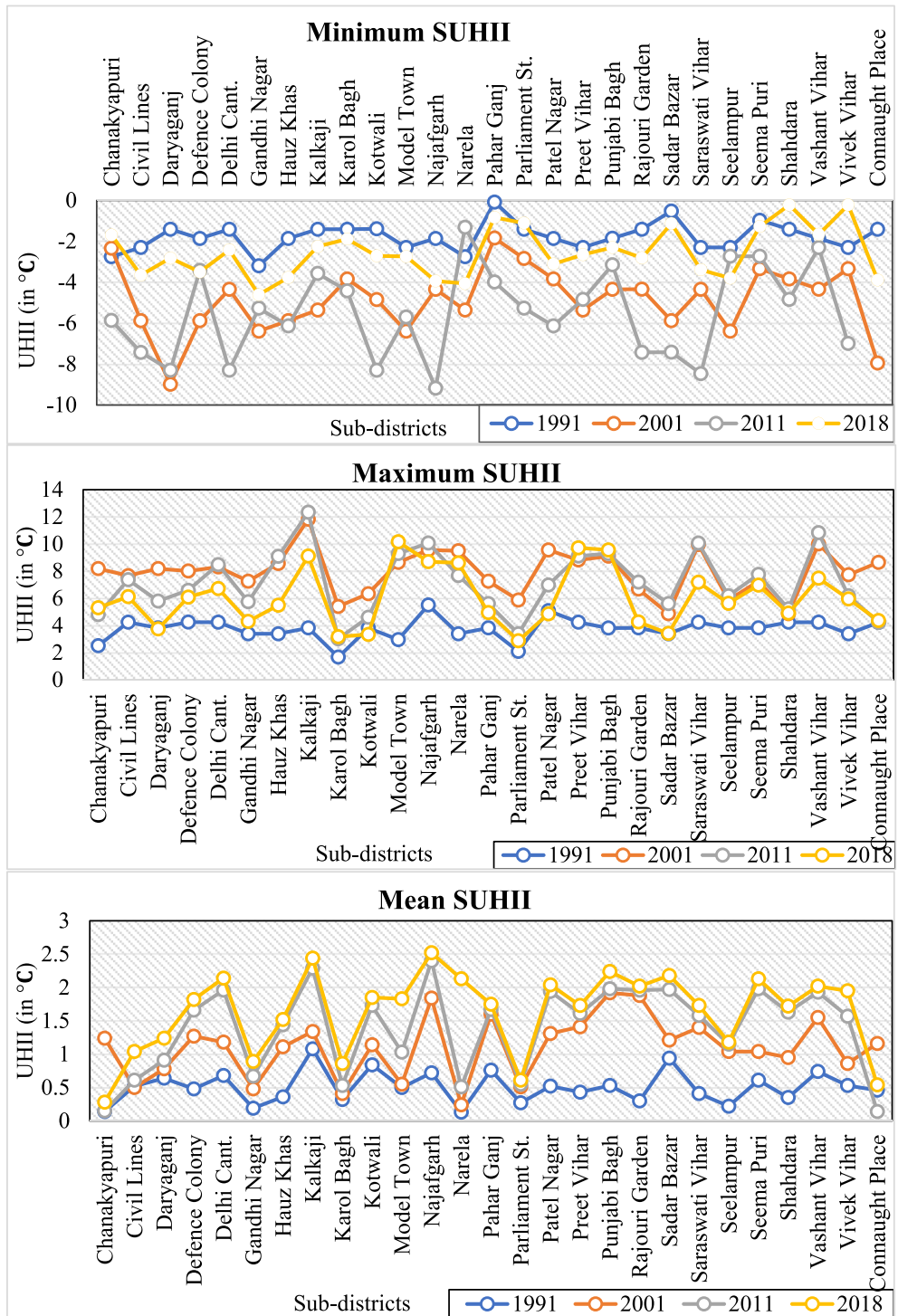


**Fig. 7.** Sub-district wise variation in statistics of SUHII in Delhi.

had experienced a very high increase in the mean SUHII ( $\geq 2^{\circ}\text{C}$ ) during 1991–2018 (Fig. 7). On the other hand, the sub-districts of the core part, like Kotwali, Chanakyapuri, Connaught Place, Sadar Bazar and Karol Bagh has experienced a very low increase in SUHII ( $<1^{\circ}\text{C}$ ).

#### 4.4. Variation in urban thermal comfort

The delineation of urban thermal comfort is used to identify the level of thermal comfort and discomfort within an urban area (Silva and Hirashima, 2021). The analysis of UTFVI shows that the thermal comfort zones have fluctuation in increase and decrease and their spatial distribution has also the dynamic pattern in Delhi during 1991–2018. The excellent and worst category thermal comfort zones are the most dominant thermal comfort zones for all the study years in Delhi (Fig. 8). The worst category thermal comfort zones were distributed in all parts of Delhi in 1991, although its concentration was more in the southern and central sub-districts. During 2001 and 2011, the concentration of worst category thermal comfort zones increased in the southern sub-districts while it declined from the western and northern sub-districts. Further, in 2018, the worst category thermal comfort zones declined from the central sub-districts and increased in the northern, southern and south-western sub-districts like in Narela, model town, Najafgarh and Hauz Khas. The statistics of UTFVI shows that the area under excellent and worst category thermal comfort zones has not experienced much change but has varied during 1991–2018.

The total area under the excellent category thermal comfort zones were about 45% of the total area in 1991 which increased to

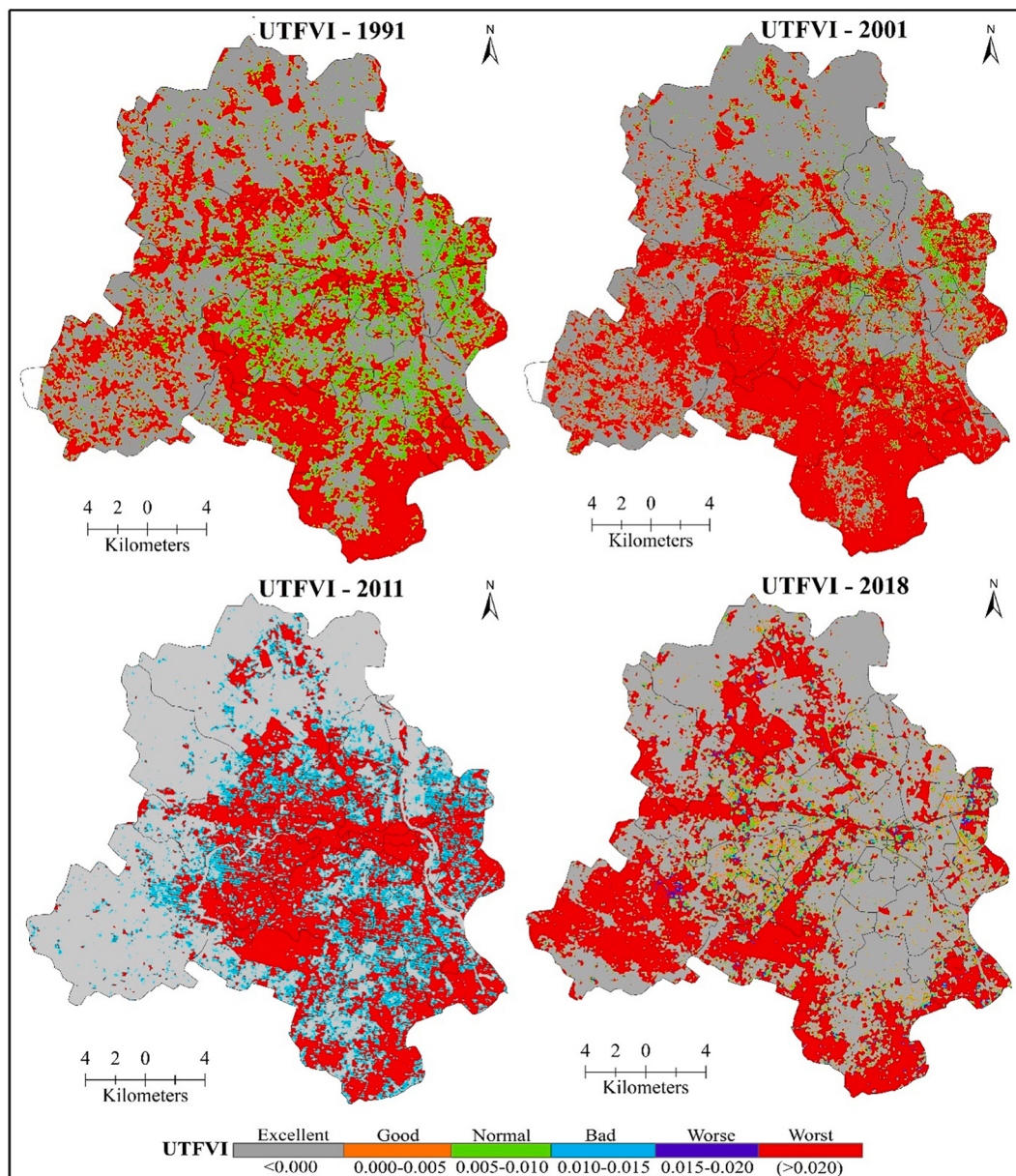


**Fig. 8.** Ecological evaluation index (EEI) of Delhi based on UTFVI.

more than 50% in 2018. At the same time, the area under the worst category thermal comfort zones were about 38% of the total area in 1991 which declined to about 36% in 2018. The reason behind low variation in thermal comfort zones and decline in the worst category thermal comfort zones is the increase in vegetation cover and scrublands in Delhi, which has been discussed earlier. On the other hand, normal category thermal comfort zones experienced a maximum decline in the area under it from about 16% to 3.50% during 1991–2018, most of which gets transferred to the bad and worse category thermal comfort zones ([Table 4](#)).

#### 4.5. Relationship between LU/LC and SUHII

The relationships between UHII and LU/LC pattern has been analyzed using the GWR model. [Fig. 9](#) exhibits the spatial distribution of  $R^2$  of the GWR model in Delhi during 1991–2018. The distribution of  $R^2$  value shows that during 1991 and 2001 shows that the relationship between LU/LC and SUHII was highest in the northern and western parts, especially in the Narela, Saraswati Vihar, Punjabi Bagh and Najafgarh sub-districts while it was low in the eastern and central parts. On the other hand, in 2001 and 2018, the association between LU/LC and SUHII increased in the southern parts of Delhi like in Hauz Khas, Kalkaji and Defence Colony sub-districts. The GWR diagnostics show that the overall regression between LU/LC and SUHII was significant for 1991, 2011 and 2018 with  $R^2$  value of 0.49, 0.51 and 0.52, respectively and adjusted  $R^2$  value of 0.45, 0.35 and 0.37, respectively. On the other hand, the overall regression was comparatively low and moderate for 2001 with  $R^2$  value of 0.39 and an adjusted  $R^2$  value of 0.21. The  $R^2$  value

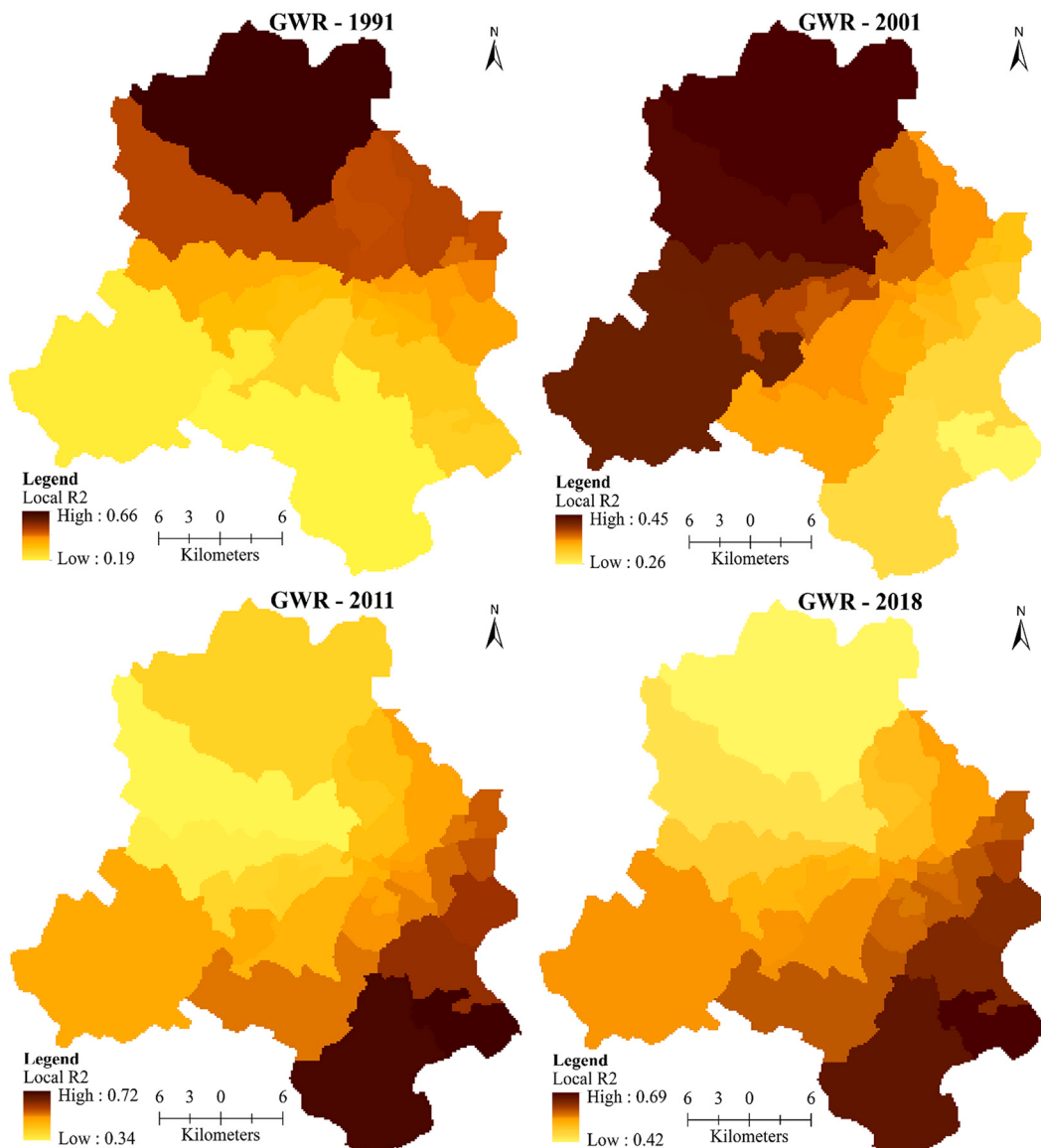


**Fig. 9.** Distribution of local  $R^2$  of the GWR model.

was low for 2001 because the error (residual square) was high in 2001 (Table 8).

The AICc value is used to assess the performance of the model used, and a lower AICc value reflects the better performance of the statical model (Brewer et al., 2016). In this study, the AICc value of the GWR model shows that the performance of the GWR model was better during 1991, 2011 and 2018 than in 2001. The coefficient of the GWR analysis is similar for all the LU/LC types and varies between -0.19 to 0.30 (Fig. 10). It means all LU/LC types have the almost same consistency in controlling the SUHII. At the same time, the Local R2 for each LU/LC type shows a varying regression coefficient for the LU/LC types during 1991–2018. The Local R2 between SUHII and built-up area shows an increasing trend during 1991–2018 but the Local R2 between other LU/LC parameters and SUHII shows a varying trend (Fig. 11). Overall, the cropland, vegetation cover and built-up area show a more consistent relationship with SUHII than other LU/LC types.

## 5. Discussion

The rapid population growth and the associated expansion of the urban areas have been recognized as the primary agents of climate change in the cities of developing countries (Zhao, 2018). It is seen in this study that the rate of urbanization in Delhi was fast during the last three decades about 21% to about 48% increase in built-up area during 1991–2018. This rapid increase in built-up surfaces in Delhi can be directly linked to the economic development and expansion of the real estate sector in Delhi and its surrounding, especially after the economic reforms of 1991 (Naikoo et al., 2020; Jain et al., 2016). Further, it was noticed that the expansion of urban areas has mostly occurred over the cropland and open lands. In the process of urbanization, the expansion of the built-up area over croplands has also been noted from the other Indian metropolitan cities such as Hyderabad (Rahman et al., 2011), Kolkata (Sahana et al., 2018) and Mumbai (Shahfahad et al., 2021a). Another important aspect of LU/LC change in Delhi during 1991–2018 was that the cropland and scrublands were firstly changed into open land and then into the built-up area. This is because the agricultural land other lands acquired by the real estate firms are left open for several years before being converted into the built-up land.

The urbanization induced increase in local warming has been reported from the many cities of developing countries (Wang and Yan, 2016; Chun and Guldmann, 2014; Zhou et al., 2004). In Delhi, although the minimum, maximum and mean LST showed a significant increase during 1991–2018, the maximum and mean LST showed a fluctuating pattern of increase and decrease. A similar pattern of fluctuation was noticed in the case of minimum and maximum SUHII during 1991–2018. The fluctuation in the statistics of SUHII and LST can be linked to the dynamics of increase and decrease in vegetation cover in Delhi. The Forest Department (2014) reported that the vegetation cover in Delhi experienced a significant increase during 1995–2015, especially in the central parts of Delhi. This led to a significant decline in SUHII and LST in Delhi. Recently, a report from The New Indian Express (2021) pointed that during 2016–2020, the central part of Delhi had lost a significant proportion of its vegetation cover. The result of this study shows that, although the statistics of SUHII and LST experienced fluctuation in increase and decrease, spatially, the high SUHII and LST increased in almost all the subdistricts, including the central sub-districts where the vegetation cover has declined during the last few years.

Evidence from literature survey shows that the core parts of the cities experienced maximum increase in SUHII because the core areas are generally densely populated with high density of built-up surface (Dewan et al., 2021; Shahfahad et al., 2021a; Atasoy, 2020). Contrary to this, in this study, the analysis of variation in SUHII showed that the SUHII has experienced a comparatively higher increase in the peripheral areas like Narela, Saraswati Vihar and Najafgarh sub-districts than the sub-districts of central parts. The higher increase in SUHII in the peripheral areas of Delhi can be linked to the large-scale transformation of croplands and scrublands to the built-up surfaces in these parts. Furthermore, the peripheral areas of Delhi have open surfaces in the form of exposed rocks of Aravalli ranges (Hang and Rahman, 2018), which have higher heat observing capacity. Because of this, the SUHII and LST are higher in the parts of southern and southwestern Delhi in comparison to the central parts. This result is similar to the results of Singh et al. (2014), who also noted strong SUHI in the outer parts of Delhi while weak SUHI in the central parts. The result also revealed that the sub-districts with a high built-up proportion in 1991 shows a high increase in minimum SUHII while a low increase in mean and maximum SUHII. On the other hand, the sub-districts in which the proportion of built-up area was low in 1991 and has increased during 2001, 2011 and 2018 shows a high increase in mean and maximum SUHII. This is because the SUHII was already higher in the already developed areas while it was low and increased during the time in the newly developed areas.

The results obtained in this study on LU/LC change and SUHII showed that the SUHII has significantly increased across all the sub-districts of Delhi which has resulted in the deteriorating thermal comfort of the city. The result of this study is similar to the previous studies (Dutta et al., 2021; Hang and Rahman, 2018), although, the previous studies did not evaluate the thermal comfort of Delhi in relation to LU/LC change. At the same time, most of the studies on other cities of India were also focused on monitoring the urban heat island and the factors behind it. In this study, we have analyzed the thermal comfort of Delhi along with the changing SUHII dynamics due to LU/LC change which is the main novelty of this study.

From the analysis of the results, it is seen that the SUHII has maximum increase at the sub-districts level which has the lowest

**Table 8**  
GWR diagnostics.

Year	Residual squares	Effective number	Sigma	AICc	R <sup>2</sup>	Adjusted R <sup>2</sup>
1991	1.209	7.959	0.252	19.060	0.49	0.45
2001	4.029	7.014	0.449	49.295	0.39	0.21
2011	5.629	9.912	0.574	66.978	0.51	0.35
2018	4.620	8.941	0.506	58.073	0.53	0.37

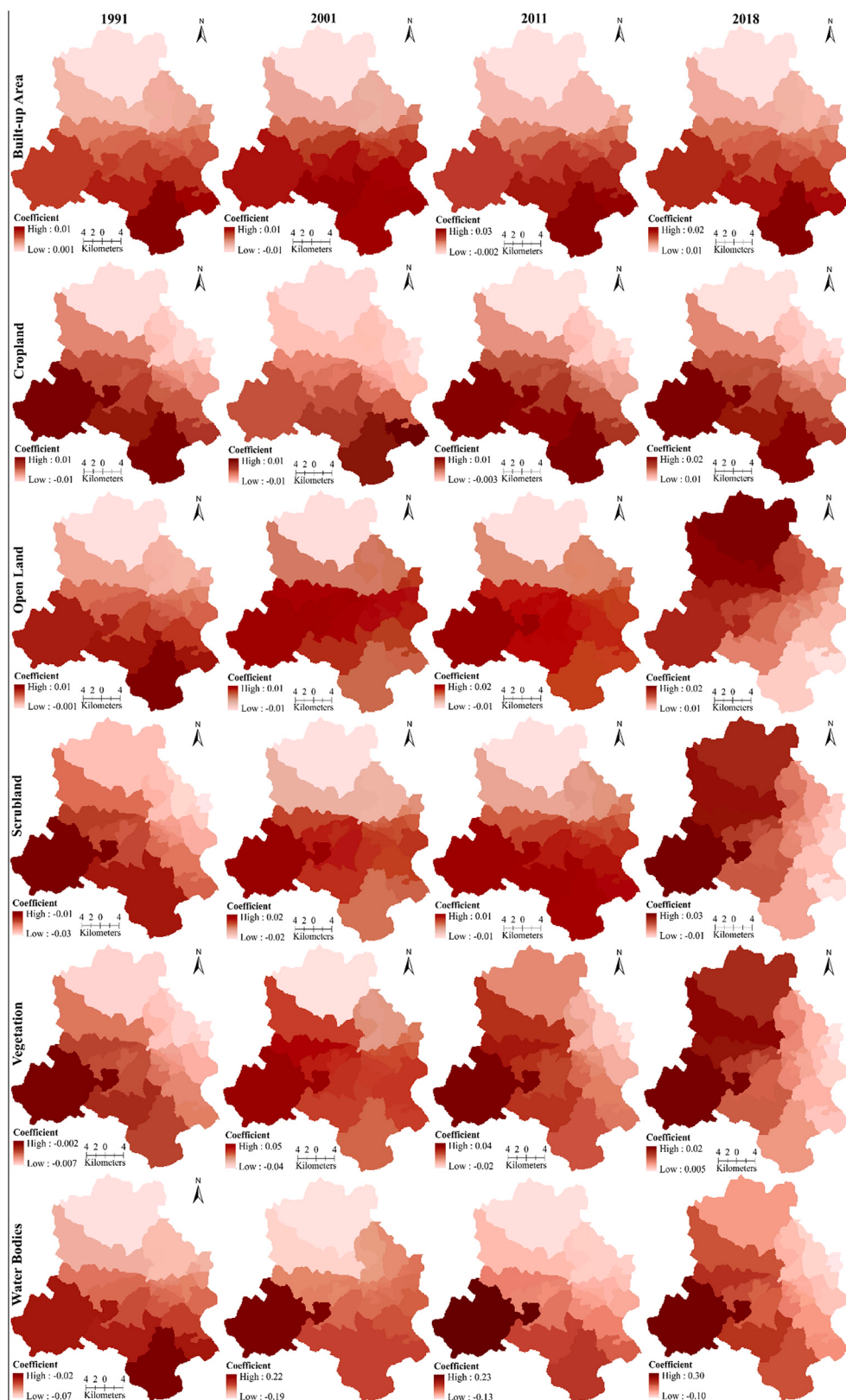


**Fig. 10.** Coefficient of the GWR between UHII and LU/LC types.

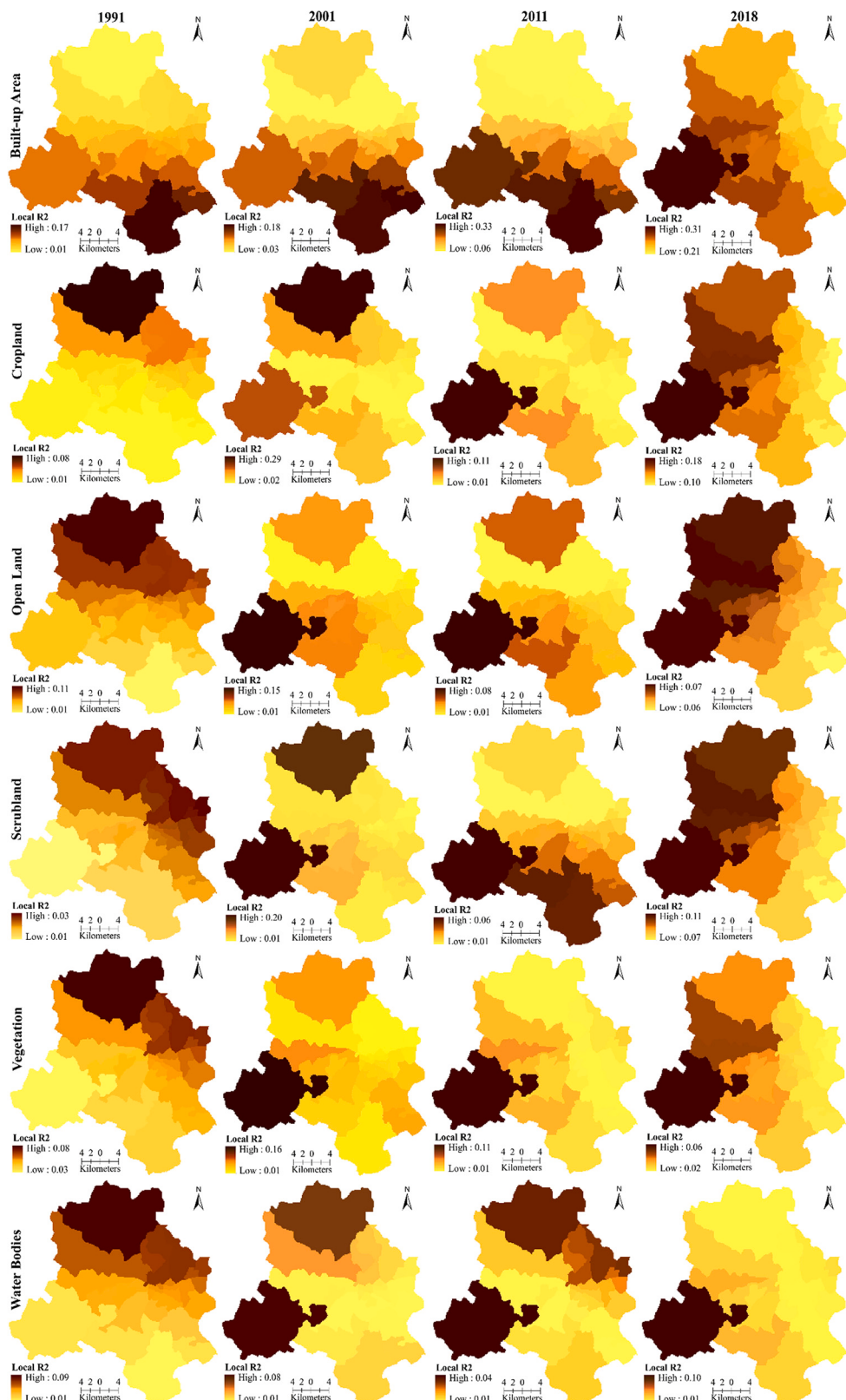


**Fig. 11.** Local R<sup>2</sup> for the GWR between UHII and LU/LC types.

vegetation cover and scrublands as well as have experienced very high built-up surfaces. Furthermore, it is seen that SUHII is comparatively low in the eastern parts of Delhi, although it has the highest built-up density. This is because of the Yamuna River, which flows in the eastern part from north to south and put a diminishing impact on the SUHI. Hence, it is suggested to make provision for the plantation of adequate vegetation cover and provision of water bodies in other parts of Delhi, where the developmental works are in process and the urban expansion is highest. This will not only provide useful insights for the SUHI mitigation but also improve the thermal comfort and ecosystem services in the city. The findings of this study can also be incorporated in the master plan of Delhi for the provision of green and blue spaces in the developing areas for SUHI mitigation and improving the quality of life. The main limitation of this study is that although, this study provides good description of the SUHII variability and its association with the LU/LC pattern, the impact of spatial arrangement of LU/LC pattern on SUHII is still not very clear, it needs to be further analyzed. Also, an annual or time series analysis of SUHII of Delhi may provide a more precise picture of the SUHII variability in Delhi with respect to LU/LC change.

## 6. Conclusion

The analysis of LU/LC change and its impacts on SUHII and urban thermal comfort of Delhi showed that the SUHII has significantly increased in Delhi during 1991–2018. The built-up area has increased to more than double during 1991–2018 while the cropland and scrublands have declined by more than half of the total area in 1991. This has significantly altered the SUHII pattern in Delhi. The area under no SUHII and category has declined from 6.70% to 3.36% while under low SUHII it increased from and 16.31% to 26.11% of the total area during 1991–2018. Similarly, the area under moderate, high and very high SUHII had increased from 1.24% to 11.56%, 0.01% to 5.75% and 0% to 3.56%, respectively. Overall, the maximum, minimum and mean SUHII has increased by 1.26 °C, 4.6 °C and 1.18 °C during 1991–2018, respectively. A similar pattern of increase and decrease has been noted in the UTFVI based analysis of urban thermal comfort. The area under excellent, good and normal thermal comfort zones has declined while it has increased under the bad, worse and worst categories thermal comfort zones. The study showed that the SUHII has experienced a maximum increase in the peripheral sub-districts like in south-western and northern sub-districts which has experienced the maximum expansion of the urban area. This is because, the expansion of the urban area in these sub-districts has occurred at the cost of vegetation cover, scrublands and croplands. At the same time, the SUHII is low in the eastern sub-districts and the change in SUHII is also very low in comparison to other parts because this part of Delhi has experienced very low changes in the LU/LC pattern and the Yamuna River flows through this part which puts diminishing effects on the SUHII. To quantify the impact of LU/LC changes on SUHII and urban thermal comfort, the GWR technique was applied which showed that the LU/LC pattern has significant impacts on the SUHII. The most interesting finding of this study is that the LST was not only higher over the built-up area but also over the open surfaces in Delhi. Finally, the study concludes that the LU/LC change has significantly changed the pattern of LST & SUHII and urban thermal comfort of Delhi.

The increasing SUHII has significantly affected the thermal comfort and urban environmental quality of Delhi. In this regard, this study can be beneficial for the mitigation of rising SUHII as well as improving the urban environmental quality. The increasing urban population and associated LU/LC change has played a crucial role in increasing the SUHII of Delhi during past few decades. Therefore, there is an urgent need of the mitigating the rising SUHII as well as its adverse impacts on population and environment. The most efficient measure for controlling the rising SUHII phenomenon and reducing its adverse impacts is the expansion of urban green cover especially in the newly developing areas of peripheral sub-districts which are experiencing very high increase in SUHII. Further, promoting the green roof technology with the goal of enhancing radiation absorption as well as construction of urban garden can also help in coping the adverse impacts of SUHII. For the further researches, it is suggested to analyze the SUHII variability concerning the number of industries, vehicular traffic, wind speed as well as atmospheric pollution in a city. Further, the procedure adopted in this study can be utilized for the analysis of SUHII and urban thermal comfort of the other cities of the world and can be further improved to overcome the main limitation that occurred in this study i.e. the satellite temperature can be integrated with the meteorological temperature for a better and more accurate analysis of the SUHII.

## Author contributions

**Shahfahad:** Conceptualization, Methodology, Software and Writing - Original draft preparation. **Mohd Waseem Naikoo:** Data analysis, Validation and Visualization. **Abu Reza Md. Towfiqul Islam:** Analysis and, Writing: editing. **Javed Mallick:** Validation, Investigation and Visualization. **Atiqur Rahman:** Supervision, Writing- Reviewing and Editing.

## Declaration of Competing Interest

The authors declare that they have no conflict of interest on any issue.

## Acknowledgement

The first and second authors are thankful to the University Grant Commission (UGC), India for providing Senior Research Fellowship (SRF) to carry out the doctoral research. All Authors are also thankful to the King Khalid University for the research collaboration and support. Thanks are also due to the USGS Earth Explorer for making Landsat data freely available to carry out this research. The authors are also thankful to the anonymous reviewers and the editor for giving scholarly comments which helped to improve the manuscript significantly.

## Appendix A. Supplementary data

Supplementary data to this article can be found online at <https://doi.org/10.1016/j.uclim.2021.101052>.

## References

- Akbari, H., Menon, S., Rosenfeld, A., 2009. Global cooling: increasing world-wide urban albedos to offset CO<sub>2</sub>. *Clim. Chang.* 94, 275–286.
- Ali, S.B., Patnaik, S., 2018. Thermal comfort in urban open spaces: objective assessment and subjective perception study in tropical city of Bhopal, India. *Urban Clim.* 24, 954–967.
- Ali, G., Abbas, S., Qamer, F.M., Wong, M.S., Rasul, G., Irteza, S.M., Shahzad, N., 2021. Environmental impacts of shifts in energy, emissions, and urban heat island during the COVID-19 lockdown across Pakistan. *J. Clean. Prod.* 291, 125806.
- Al-Kafy, A., Rahman, M.S., Hasan, M.M., Islam, M., 2020. Modelling future land use land cover changes and their impacts on land surface temperatures in Rajshahi, Bangladesh. *Remote Sens. Appl. Soc. Environ.* 18, 100314.
- Alqaesmi, A.S., Hereher, M.E., Kaplan, G., Al-Quraishi, A.M.F., Saibi, H., 2021. Impact of COVID-19 lockdown upon the air quality and surface urban heat island intensity over the United Arab Emirates. *Sci. Total Environ.* 767, 144330.
- Artis, D.A., Carnahan, W.H., 1982. Survey of emissivity variability in thermography of urban areas. *Remote Sens. Environ.* 12 (4), 313–329.
- Atasoy, M., 2020. Assessing the impacts of land-use/land-cover change on the development of urban heat island effects. *Environ. Dev. Sustain.* 22, 7547–7557.
- Aylett, A., Joeman, B.D., Lefevre, B., Luque-Ayala, A., Rahman, A., Roberts, D., Ward, S., Watkins, M., 2016. Climate change mitigation in rapidly developing cities. In: Seto, K.C., et al. (Eds.), *The Routledge Handbook of Urbanization and Global Environmental Change*. Routledge, Abingdon, pp. 549–560.
- Baviskar, A., 2011. Spectacular events, City spaces and citizenship: The commonwealth games in Delhi. In: Anjaria, J.E., McFarlane, C. (Eds.), *Urban Navigations: Politics, Space and the City in South Asia*. Routledge, New Delhi, pp. 138–161.
- Bechtel, B., Demuzere, M., Mills, G., Zhan, W., Sismanidis, P., Small, C., Voogt, J., 2019. SUHI analysis using Local Climate Zones—a comparison of 50 cities. *Urban Clim.* 28, 100451.
- Brewer, M.J., Butler, A., Cooksley, S.L., 2016. The relative performance of AIC, AICC and BIC in the presence of unobserved heterogeneity. *Methods Ecol. Evol.* 7 (6), 679–692.
- Buo, I., Sagris, V., Burdun, I., Uuemaa, E., 2021. Estimating the expansion of urban areas and urban heat islands (UHI) in Ghana: a case study. *Nat. Hazards* 105, 1299–1321.
- Cao, C., Lee, X., Liu, S., et al., 2016. Urban heat islands in China enhanced by haze pollution. *Nat. Commun.* 7, 12509.
- Census of India, 2011. N.C.T of Delhi Series-08 Part XII-B District Census Handbook of all the Nine Districts. Directorate of Census Operations, Delhi. [https://www.censusindia.gov.in/2011census/dchb/0700\\_PART\\_B\\_DCHB\\_0700\\_NCT%20OF%20DELHI.pdf](https://www.censusindia.gov.in/2011census/dchb/0700_PART_B_DCHB_0700_NCT%20OF%20DELHI.pdf).
- Chadchan, J., Shankar, R., 2012. An analysis of urban growth trends in the post-economic reforms period in India. *Int. J. Sustain. Built Environ.* 1, 36–49.
- Chakraborty, T.C., Sarangi, C., Lee, X., 2021. Reduction in human activity can enhance the urban heat island: insights from the COVID-19 lockdown. *Environ. Res. Lett.* 16, 054060.
- Chatterjee, S., Khan, A., Dinda, A., Mithun, S., Khatun, R., Akbari, H., Kusaka, H., Mitra, C., Bhatti, S.S., Doan, Q.V., Wang, Y., 2019. Simulating micro-scale thermal interactions in different building environments for mitigating urban heat islands. *Science of the Total environment.* *Sci. Total Environ.* 663, 610–631.
- Chaudhry, P., Bagra, K., Singh, B., 2011. Urban greenery status of some Indian cities: a short communication. *Int. J. Environ. Sci. Dev.* 2 (2), 98.
- Chun, B., Guldmann, J.M., 2014. Spatial statistical analysis and simulation of the urban heat island in high-density central cities. *Landscape. Urban Plan.* 125, 76–88.
- Corburn, J., 2009. Cities, climate change and urban Heat Island mitigation: localising global environmental science. *Urban Stud.* 46 (2), 413–427.
- Dewan, A., Kiselev, G., Botje, D., Mahmud, G.I., Bhuiyan, M.H., Hassan, Q.K., 2021. Surface urban heat island intensity in five major cities of Bangladesh: patterns, drivers and trends. *Sustain. Cities Soc.* 71, 102926.
- Du, P., Chen, J., Bai, X., Han, W., 2020. Understanding the seasonal variations of land surface temperature in Nanjing urban area based on local climate zone. *Urban Clim.* 33, 100657.
- Dutta, D., Rahman, A., Paul, S.K., Kundu, A., 2021. Impervious surface growth and its inter-relationship with vegetation cover and land surface temperature in peri-urban areas of Delhi. *Urban Climate* 37, 100799.
- Estoque, R.C., Murayama, Y., Myint, S.W., 2016. Effects of landscape composition and pattern on land surface temperature: an urban heat island study in the megacities of Southeast Asia. *Sci. Total Environ.* 577, 349–359.
- Fan, C., Myint, S.W., Kaplan, S., Middel, A., Zheng, B., Rahman, A., Huang, H.P., Brazel, A., Blumberg, D.G., 2017. Understanding the impact of urbanization on surface urban heat islands—a longitudinal analysis of the oasis effect in subtropical desert cities. *Remote Sens.* 9 (7), 672.
- Forest Department, 2014. Extent of Forest and Tree Cover. Government of National Capital Territory of Delhi, India. [http://forest.delhigovt.nic.in/wps/wcm/connect/doit\\_forest/Forest/Home/Forests+of+Delhi/](http://forest.delhigovt.nic.in/wps/wcm/connect/doit_forest/Forest/Home/Forests+of+Delhi/).
- Fotheringham, A.S., Brunsdon, C., Charlton, M., 2003. Geographically weighted regression: the analysis of spatially varying relationships. John Wiley & Sons.
- Giridharan, R., Emmanuel, R., 2018. The impact of urban compactness, comfort strategies and energy consumption on tropical urban heat island intensity: A review. *Sustain. Cities Soc.* 40, 677–687.
- Guha, S., Govil, H., Dey, A., Gill, N., 2018. Analytical study of land surface temperature with NDVI and NDBI using Landsat 8 OLI and TIRS data in Florence and Naples city, Italy. *European Journal of Remote Sensing* 51 (1), 667–678.
- Halder, B., Bandyopadhyay, J., Banik, P., 2021. Monitoring the effect of urban development on urban heat island based on remote sensing and geo-spatial approach in Kolkata and adjacent areas, India. *Sustain. Cities Soc.* 74, 103186.
- Hang, H.T., Rahman, A., 2018. Characterization of thermal environment over heterogeneous surface of National Capital Region (NCR), India using LANDSAT-8 sensor for regional planning studies. *Urban Clim.* 24, 1–18.
- Heaviside, C., Macintyre, H., Vardoulakis, S., 2017. The urban Heat Island: implications for health in a changing environment. *Curr. Environ. Health Rep.* 4, 296–305.
- Hersperger, A.M., Oliveira, E., Pagliarin, S., Palka, G., Verburg, P., Bolliger, J., Grädinaru, S., 2018. Urban land-use change: the role of strategic spatial planning. *Glob. Environ. Chang.* 51, 32–42.
- Jain, M., Dimri, A.P., Niyogi, D., 2016. Urban sprawl patterns and processes in Delhi from 1977 to 2014 based on remote sensing and spatial metrics approaches. *Earth Interact.* 20, 1–28.
- Kumari, P., Kapur, S., Garg, V., Kumar, K., 2020a. Effect of surface temperature on energy consumption in a calibrated building: a case study of Delhi. *Climate* 8 (6), 71.
- Kumari, B., Tayyab, M., Ahmed, I.A., Baig, M.R.I., Khan, M.F., Rahman, A., 2020b. Longitudinal study of land surface temperature (LST) using mono-and split-window algorithms and its relationship with NDVI and NDBI over selected metro cities of India. *Arab. J. Geosci.* 13 (19), 1–19.
- Kumari, B., Shahfahad, Tayyab, M., Ahmed, I.A., Baig, M.R.I., Ali, M.A., Asif, Usmani, T.M., Rahman, A., 2021. Land use/land cover (LU/LC) change dynamics using indices overlay method in Gautam Buddha Nagar District-India. *GeoJournal.* <https://doi.org/10.1007/s10708-021-10374-w>.
- Lee, T.W., Lee, J.Y., Wang, Z.H., 2012. Scaling of the urban heat island intensity using time-dependent energy balance. *Urban Clim.* 2, 16–24.
- Li, H., Zhou, Y., Li, X., Meng, L., Wang, X., Wu, S., Sodoudi, S., 2018. A new method to quantify surface urban heat island intensity. *Sci. Total Environ.* 624, 262–272.
- Lu, L., Weng, Q., Xiao, D., Guo, H., Li, Q., Hui, W., 2020. Spatiotemporal variation of surface urban heat islands in relation to land cover composition and configuration: A multi-scale case study of Xi'an, China. *Remote Sensing* 12 (17), 2713.

- Ma, Y., Kuang, Y., Huang, N., 2010. Coupling urbanization analyses for studying urban thermal environment and its interplay with biophysical parameters based on TM/ETM+ imagery. *Int. J. Appl. Earth Obs. Geoinf.* 12 (2), 110–118.
- Mallick, J., Rahman, A., Singh, C.K., 2013. Modeling urban heat islands in heterogeneous land surface and its correlation with impervious surface area by using night-time ASTER satellite data in highly urbanizing city, Delhi-India. *Adv. Space Res.* 52 (4), 639–655.
- McDonald, R.I., Marcotullio, P.J., Güneralp, B., 2013. Urbanization and global trends in biodiversity and ecosystem services. In: *Urbanization, Biodiversity and Ecosystem Services: Challenges and Opportunities*. Springer, Dordrecht, pp. 31–52.
- Meng, Y., Yang, M., Liu, S., Mou, Y., Peng, C., Zhou, X., 2021. Quantitative assessment of the importance of bio-physical drivers of land cover change based on a random forest method. *Ecol. Inform.* 61, 101204.
- Mohan, M., Kikegawa, Y., Gurjar, B.R., Bhati, S., Kolli, N.R., 2013. Assessment of urban heat island effect for different land use–land cover from micrometeorological measurements and remote sensing data for megacity Delhi. *Theor. Appl. Climatol.* 112 (3), 647–658.
- Munslow, B., O'Dempsey, T., 2010. Globalisation and climate change in Asia: the urban health impact. *Third World Q.* 31 (8), 1339–1356.
- Naikoo, M.W., Rihan, M., Ishtiaq, M., Shahfahad, , 2020. Analyses of land use land cover (LULC) change and built-up expansion in the suburb of a metropolitan city: spatio-temporal analysis of Delhi NCR using Landsat datasets. *J. Urban Manag.* 9 (3), 347–359.
- Naim, M.N.H., Kafy, A.A., 2021. Assessment of urban thermal field variance index and defining the relationship between land cover and surface temperature in Chattogram city: a remote sensing and statistical approach. *Environ. Challeng.* 4, 100107.
- Oke, T.R., 1973. City size and the urban heat island. *Atmos. Environ.* 7, 769–779.
- Panagopoulos, T., Duque, J.A.G., Dan, M.B., 2016. Urban planning with respect to environmental quality and human well-being. *Environ. Pollut.* 208, 137–144.
- Pandey, A.K., Singh, S., Berwal, S., Kumar, D., Pandey, P., Prakash, A., Kumar, K., 2014. Spatio-temporal variations of urban heat island over Delhi. *Urban Clim.* 10, 119–133.
- Paul, S., Nagendra, H., 2015. Vegetation change and fragmentation in the mega city of Delhi: mapping 25 years of change. *Appl. Geogr.* 58, 153–166.
- Qin, Z., Karnieli, A., Berliner, P., 2001. A mono-window algorithm for retrieving land surface temperature from Landsat TM data and its application to the Israel-Egypt border region. *Int. J. Remote Sens.* 22 (18), 3719–3746.
- Rahman, A., Kumar, Y., Fazal, S., Bhaskaran, S., 2011. Urbanization and quality of urban environment using remote sensing and GIS techniques in East Delhi-India. *J. Geogr. Inf. Syst.* 3, 61–83.
- Rajan, E.H.S., Amirtham, L.R., 2021. Urban heat island intensity and evaluation of outdoor thermal comfort in Chennai, India. *Environ. Dev. Sustain.* <https://doi.org/10.1007/s10668-021-01344-w>.
- Ramaiah, M., Avtar, R., 2019. Urban green spaces and their need in cities of rapidly urbanizing India: a review. *Urban Sci.* 3 (3), 94.
- Sahana, S., Hong, H., Sajjad, H., 2018. Analyzing urban spatial patterns and trend of urban growth using urban sprawl matrix: a study on Kolkata urban agglomeration, India. *Sci. Total Environ.* 628–629, 1557–1566.
- Sahoo, S.K., Himesh, S., Gouda, K.C., 2020. Impact of urbanization on heavy rainfall events: a case study over the megacity of Bengaluru, India. *Pure Appl. Geophys.* 177, 6029–6049.
- Seto, K.C., Güneralp, B., Hutyra, L.R., 2012. Global forecasts of urban expansion to 2030 and direct impacts on biodiversity and carbon pools. *Proc. Natl. Acad. Sci.* 109 (40), 16083–16088.
- Shahfahad, Talukdar, S., Rihan, M., Hang, H.T., Bhaskaran, S., Rahman, A., 2021a. Modelling urban heat island (UHI) and thermal field variation and their relationship with land use indices over Delhi and Mumbai metro cities. *Environ. Dev. Sustain.* <https://doi.org/10.1007/s10668-021-01587-7>.
- Shahfahad, Rihan, M., Naikoo, M.W., Ali, M.A., Usmani, T.M., Rahman, A., 2021b. Urban Heat Island dynamics in response to land-use/land-cover change in the Coastal City of Mumbai. *J. Indian Soc. Remote Sens.* <https://doi.org/10.1007/s12524-021-01394-7>.
- Sharma, R., Pradhan, L., Kumari, M., Bhattacharya, P., 2021. Assessing urban heat islands and thermal comfort in Noida City using geospatial technology. *Urban Clim.* 35, 100751.
- Silva, T.J.V., Hirashima, S.Q.S., 2021. Predicting urban thermal comfort from calibrated UTCI assessment scale - a case study in Belo Horizonte city, southeastern Brazil. *Urban Clim.* 36, 100652.
- Singh, R.B., Grover, A., Zhan, J., 2014. Inter-seasonal variations of surface temperature in the urbanized environment of Delhi using Landsat thermal data. *Energies* 7, 1811–1828.
- Sobrino, J.A., Jiménez, C.J., Paolini, M., 2004. Land surface temperature retrieval from LANDSAT TM 5. *Remote Sens. Environ.* 90, 434–440.
- Stewart, I.D., Oke, T.R., 2012. Local climate zones for urban temperature studies. *Bull. Am. Meteorol. Soc.* 93 (12), 1879–1900.
- Talukdar, S., Singha, P., Mahato, S., Shahfahad, Pal, S., Liou, Y.A., Rahman, A., 2020. Land-use land-cover classification by machine learning classifiers for satellite observations—A review. *Remote Sens.* 12 (7), 1135.
- The New Indian Express, 2021. Continuous Loss of Green Cover in Recent Years a Concern for NDMC. <https://www.newindianexpress.com/cities/delhi/2021/jul/29/continuous-loss-of-green-cover-in-recent-years-a-concern-for-ndmc-2337073.html>.
- Ünal, Y.S., Sonuç, C.Y., Incecik, S., Topcu, H.S., Diren-Üstün, D.H., Temizöz, H.P., 2019. Investigating urban heat island intensity in Istanbul. *Theor. Appl. Climatol.* 139 (1–2), 175–190.
- Wang, Y., Akbari, H., 2016. The effects of street tree planting on urban Heat Island mitigation in Montreal. *Sustain. Cities Soc.* 27, 122–128.
- Wang, J., Yan, Z.-W., 2016. Urbanisation related warming in local temperature records: a review. *Atmos. Ocean Sci. Lett.* 9 (2), 129–138.
- Ward, K., Lauf, S., Kleinschmit, B., Endlicher, W., 2016. Heat waves and urban heat islands in Europe: a review of relevant drivers. *Sci. Total Environ.* 569–570, 527–539.
- Wentz, E., Nelson, D., Rahman, A., Stefanov, W., Roy, S.S., 2008. Expert system classification of urban land use/cover for Delhi, India. *Int. J. Remote Sens.* 29 (15), 4405–4427.
- WUP, 2018–2019. World Urbanization Prospects 2018 – Highlights. Department of Economic and Social Affairs Population Division, United Nations, New York. <https://population.un.org/wup/Publications/Files/WUP2018-Highlights.pdf>.
- Xu, L.Y., Xie, X.D., Li, S., 2013. Correlation analysis of the urban heat island effect and the spatial and temporal distribution of atmospheric particulates using TM images in Beijing. *Environ. Pollut.* 178, 102–114.
- Yao, R., Wang, L., Huang, X., Niu, Z., Liu, F., Wang, Q., 2017. Temporal trends of surface urban heat islands and associated determinants in major Chinese cities. *Sci. Total Environ.* 609, 742–754.
- Yao, R., Wang, L., Huang, X., Gong, W., Xia, X., 2019. Greening in rural areas increases the surface urban heat island intensity. *Geophys. Res. Lett.* 46 (4), 2204–2212.
- Yao, R., Wang, L., Huang, X., Sun, L., Chen, R., Wu, X., Niu, Z., 2021. A robust method for filling the gaps in MODIS and VIIRS land surface temperature data. *IEEE Trans. Geosci. Remote Sens.* 1–15. <https://doi.org/10.1109/TGRS.2021.3053284>.
- Yu, X., Guo, X., Wu, Z., 2014. Land surface temperature retrieval from Landsat 8 TIRS—comparison between radiative transfer equation-based method, split window algorithm and single channel method. *Remote Sens.* 6 (10), 9829–9852.
- Zawadzka, Harris, J.A., Corstanje, R., 2021. Assessment of heat mitigation capacity of urban greenspaces with the use of InVEST urban cooling model, verified with day-time land surface temperature data. *Landsc. Urban Plan.* 214, 104163.
- Zhang, Y., 2006. Land surface temperature retrieval from CBERS-02 IRMSS thermal infrared data and its applications in quantitative analysis of urban heat island effect. *J. Remote Sens.* 10, 789–797.
- Zhao, L., 2018. Urban growth and climate adaptation. *Nat. Clim. Chang.* 8, 1034.
- Zhou, L., Dickinson, R.E., Tian, Y., Fang, J., Li, Q., Kaufmann, R.K., Tucker, C.J., Myneni, R.B., 2004. Evidence for a significant urbanization effect on climate in China. *Proc. Natl. Acad. Sci. U. S. A.* 101 (26), 9540–9544.
- Zhu, K., Bayer, P., Grathwohl, P., Blum, P., 2015. Groundwater temperature evolution in the subsurface urban heat island of Cologne, Germany. *Hydrol. Process.* 29, 965–978.